

ey.9



# DEVELOPMENT OF A CRYOGENICALLY PUMPED MASS SPECTROMETER PROBE FOR ROCKET PLUME STUDIES

Mc Coy  
Ponci  
Busby

VON KÁRMÁN GAS DYNAMICS FACILITY  
ARNOLD ENGINEERING DEVELOPMENT CENTER  
AIR FORCE SYSTEMS COMMAND  
ARNOLD AIR FORCE STATION, TENNESSEE 37389

June 1976

Final Report for Period July 1, 1972 — June 30, 1975

Prop. by, AIR FORCE  
...  
140500-75-0-0001

Approved for public release; distribution unlimited.

Prepared for

DIRECTORATE OF TECHNOLOGY (DY)  
ARNOLD ENGINEERING DEVELOPMENT CENTER  
ARNOLD AIR FORCE STATION, TENNESSEE 37389

## NOTICES

When U. S. Government drawings specifications, or other data are used for any purpose other than a definitely related Government procurement operation, the Government thereby incurs no responsibility nor any obligation whatsoever, and the fact that the Government may have formulated, furnished, or in any way supplied the said drawings, specifications, or other data, is not to be regarded by implication or otherwise, or in any manner licensing the holder or any other person or corporation, or conveying any rights or permission to manufacture, use, or sell any patented invention that may in any way be related thereto.

Qualified users may obtain copies of this report from the Defense Documentation Center.

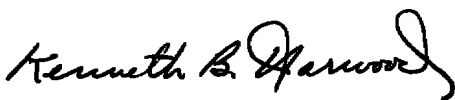
References to named commercial products in this report are not to be considered in any sense as an endorsement of the product by the United States Air Force or the Government.

This report has been reviewed by the Information Office (OI) and is releasable to the National Technical Information Service (NTIS). At NTIS, it will be available to the general public, including foreign nations.

## APPROVAL STATEMENT

This technical report has been reviewed and is approved for publication.

FOR THE COMMANDER



KENNETH B. HARWOOD  
Major, CF  
Research & Development  
Division  
Directorate of Technology



ROBERT O. DIETZ  
Director of Technology

# UNCLASSIFIED

REPORT DOCUMENTATION PAGE		READ INSTRUCTIONS BEFORE COMPLETING FORM
1 REPORT NUMBER <b>AEDC-TR-76-55</b>	2 GOVT ACCESSION NO.	3 RECIPIENT'S CATALOG NUMBER
4 TITLE (and Subtitle) <b>DEVELOPMENT OF A CRYOGENICALLY PUMPED MASS SPECTROMETER PROBE FOR ROCKET PLUME STUDIES</b>		5 TYPE OF REPORT & PERIOD COVERED <b>Final Report-July 1, 1972 - June 30, 1975</b>
		6 PERFORMING ORG. REPORT NUMBER
7 AUTHOR(s) <b>T. D. McCay and H. M. Powell, ARO, Inc. and M. R. Busby, Tennessee State University, Nashville, Tennessee</b>		8 CONTRACT OR GRANT NUMBER(s)
9 PERFORMING ORGANIZATION NAME AND ADDRESS <b>Arnold Engineering Development Center (DY) Air Force Systems Command Arnold Air Force Station, Tennessee 37389</b>		10 PROGRAM ELEMENT, PROJECT, TASK AREA & WORK UNIT NUMBERS <b>Program Element 65807F</b>
11 CONTROLLING OFFICE NAME AND ADDRESS <b>Arnold Engineering Development Center (DYFS) Arnold Air Force Station, Tennessee 37389</b>		12. REPORT DATE <b>June 1976</b>
		13. NUMBER OF PAGES <b>67</b>
14 MONITORING AGENCY NAME & ADDRESS (if different from Controlling Office)		15 SECURITY CLASS. (of this report)  <b>UNCLASSIFIED</b>
		15a. DECLASSIFICATION/DOWNGRADING SCHEDULE <b>N/A</b>
16 DISTRIBUTION STATEMENT (of this Report)  <b>Approved for public release; distribution unlimited.</b>		
17 DISTRIBUTION STATEMENT (of the abstract entered in Block 20, if different from Report)		
18 SUPPLEMENTARY NOTES  <b>Available in DDC</b>		
19 KEY WORDS (Continue on reverse side if necessary and identify by block number)  <div style="display: flex; justify-content: space-between;"> <div> <b>cryogenics</b> <b>spectrometers</b> <b>probes</b> <b>nitrogen</b> </div> <div> <b>argon</b> <b>hydrogen</b> <b>density (specie)</b> <b>rockets</b> </div> <div> <b>plumes</b> </div> </div>		
20 ABSTRACT (Continue on reverse side if necessary and identify by block number)  <p>Two cryogenically cooled (20°K) mass spectrometer probes were developed for sampling species concentrations in a rocket exhaust plume. A flat-face probe with a cryogenic (20°K) skimmer and a conical probe with a warm 20-deg half-angle conical skimmer were evaluated in room temperature free-jet expansions of nitrogen, argon, and gas mixtures containing hydrogen. Cryosorption pumping of hydrogen by 20°K CO<sub>2</sub> frosts was employed within the probes.</p>		

# UNCLASSIFIED

# UNCLASSIFIED

## 20. ABSTRACT (Continued)

Typical probe pressures were maintained on the  $10^{-7}$  torr scale. Species densities were measured in the room temperature free jets and calibrations determined. The flat-face probe was determined to be unsuitable for rocket testing. The conical probe was tested in the exhaust plume of a 1-lb thrust MMH/N<sub>2</sub>O<sub>4</sub> liquid rocket engine and major species concentrations were determined for several O/F ratios. Qualitative minor species measurements were also made.



## PREFACE

The work reported herein was conducted by the Arnold Engineering Development Center (AEDC), Air Force Systems Command (AFSC), under the sponsorship of the Defense Advanced Research Projects Agency and Headquarters, Arnold Engineering Development Center, under Program Element 65807F. The results were obtained by ARO, Inc. (a subsidiary of Sverdrup & Parcel and Associates, Inc.), contract operator of AEDC, AFSC, Arnold Air Force Station, Tennessee. This work was conducted under ARO Project Nos. VF278, VF478-13YA, and V32S-56A. The authors of this report were T. D. McCay and H. M. Powell, ARO, Inc., and M. R. Busby, consultant to ARO, Inc., and Assistant Professor of Mechanical Engineering, Tennessee State University, Nashville. The manuscript (ARO Control No. ARO-VKF-TR-75-113) was submitted for publication on June 30, 1975.

## CONTENTS

	<u>Page</u>
1.0 INTRODUCTION . . . . .	7
2.0 PROBE DESIGN	
2.1 Rocket Plume Constituents . . . . .	8
2.2 Performance Characteristics of a 75-lb- Thrust Engine. . . . .	9
2.3 Mass-Sampling Considerations . . . . .	11
2.3.1 Shock-Induced Mass Separation . . . . .	11
2.3.2 Velocity Distribution Alteration due to Shock Waves. . . . .	12
2.3.3 Internal Mass Separation . . . . .	12
2.3.4 External Scattering in Rarefied Flow . . . . .	12
2.3.5 Internal Scattering . . . . .	13
2.4 Probe Sizing and Positioning . . . . .	13
2.5 Instrumentation Design Considerations. . . . .	19
3.0 EXPERIMENTAL PROCEDURE . . . . .	20
4.0 PROBE PERFORMANCE IN COLD FLOWS	
4.1 Flat-Face Probe . . . . .	22
4.1.1 Probe-Pumping Evaluation . . . . .	22
4.1.2 Plume-Sampling: Measurements . . . . .	24
4.1.3 Calculation of Impact Pressures at Pumping Breakdown . . . . .	24
4.2 Conical-Face Probe . . . . .	25
4.2.1 Probe-Pumping Evaluation . . . . .	29
4.2.2 Plume-Sampling Measurements . . . . .	30
4.2.3 Impact Pressures at Pumping Breakdown . . . . .	30
4.3 Mass Spectrometer Performance . . . . .	33
4.3.1 Ionizer for Mass Filter Assembly . . . . .	33
4.3.2 Quadrupole Cracking Patterns . . . . .	34
4.3.3 Effects of Long RF Lines . . . . .	38
4.4 Additional Performance Considerations . . . . .	38
4.4.1 Frost Poisoning . . . . .	38
4.4.2 Diffusive Separation in Sonic Orifice Flows . . . . .	39
4.4.3 Background Gas Invasion . . . . .	39

	<u>Page</u>
5.0 SAMPLING OF A 1-LB-THRUST MMH/N <sub>2</sub> O <sub>4</sub> ROCKET ENGINE	
5.1 Chamber . . . . .	40
5.2 Probe Selection and Modification . . . . .	41
5.3 Rocket Engine . . . . .	42
5.4 Fuel and Oxidizer Systems . . . . .	44
5.5 Liquid Helium Pump . . . . .	44
5.6 Instrumentation . . . . .	49
5.6.1 Mass Spectrometer System . . . . .	49
5.6.2 PDP-8 Computer System . . . . .	50
5.7 Calibrations. . . . .	51
5.8 Chamber and Engine Performance. . . . .	52
5.9 Probe Evaluation . . . . .	53
5.9.1 Probe Pumping. . . . .	56
5.9.2 Major Species . . . . .	57
5.9.3 Minor Species . . . . .	60
5.9.4 Velocity Distributions. . . . .	61
6.0 SUMMARY AND CONCLUSIONS . . . . .	62

## ILLUSTRATIONS

### Figure

1. Schematic of Flat-Face Probe . . . . .	18
2. Schematic of Conical Probe . . . . .	18
3. Schematic of the Molecular Beam Chamber . . . . .	21
4. Schematic of 4- by 10-ft Research Vacuum Chamber . . . . .	21
5. Probe Pressure Response for No CO <sub>2</sub> Deposition . . . . .	23
6. Probe Pressure Response for CO <sub>2</sub> Deposition . . . . .	23
7. Probe Pressure versus Impact Pressure . . . . .	26
8. Flat-Face Probe Performance for Nitrogen . . . . .	26
9. Flat-Face Probe Performance for Argon . . . . .	27
10. Flat-Face Probe Performance for H <sub>2</sub> , CO, N <sub>2</sub> Mixture . . . . .	27

<u>Figure</u>	<u>Page</u>
11. Minor Specie Measurement . . . . .	28
12. Flat-Face Probe Performance for Hydrogen and Carbon Dioxide . . . . .	28
13. Conical Probe Pumping Performance. . . . .	29
14. Conical Probe Performance for Nitrogen . . . . .	31
15. N <sub>2</sub> Performance for the Conical Probe . . . . .	31
16. Conical-Face Probe Performance in a 20-percent H <sub>2</sub> , 80-percent CO <sub>2</sub> Jet. . . . .	32
17. Conical Probe Performance in a 1-percent H <sub>2</sub> , 99-percent CO <sub>2</sub> Mixture . . . . .	32
18. Mass Spectrometer, Probe and Assembly . . . . .	33
19. Ionizer Construction for the Mass Spectrometer Assembly Used in the Molecular Beam Chamber . . . . .	34
20. Schematic of 4- by 10-ft Research Vacuum Chamber and Rocket Configuration . . . . .	41
21. One-Pound Thrust Engine and Values . . . . .	42
22. Nozzle Contour of Thruster . . . . .	43
23. Schematic of Rocket Engine Propellant System . . . . .	45
24. Rocket Engine-Propellant System Installation . . . . .	46
25. Liquid Helium Pump Schematic . . . . .	48
26. Nitrogen Calibration . . . . .	53
27. Carbon Monoxide Calibration . . . . .	54
28. Hydrogen Calibration, 2,500-v Multiplier Voltage . . . . .	54
29. Hydrogen Calibration, 2,900-v Multiplier Voltage . . . . .	55
30. Vacuum Chamber Pressure Temporal Behavior . . . . .	55
31. Combustion Chamber Pressure for Three O/F Ratios . . . . .	56
32. Probe Pressure during Rocket Firings . . . . .	57

<u>Figure</u>	<u>Page</u>
33. Typical Rocket Exhaust Mass Spectra . . . . .	58
34. Variation of Species with O/F Ratio . . . . .	58
35. Minor Specie Mass Spectra. . . . .	60

## TABLES

1. Theoretical Plume Composition for Complete Combustion . . . . .	9
2. 75-lb-Thrust Rocket Engine Characteristics . . . . .	10
3. 75-lb-Thrust Engine Centerline Impact Pressure Measurements . . . . .	10
4. Design Parameters and Flow Conditions . . . . .	16
5. Methane Cracking Patterns . . . . .	36
6. Acetylene Cracking Patterns . . . . .	36
7. Ethylene Cracking Patterns . . . . .	37
8. Propylene Cracking Patterns . . . . .	37
9. One-Pound Rocket Engine Characteristics . . . . .	43
10. Rocket Constituent Heat Loads. . . . .	46
11. Measured Specie Concentrations (O/F = 1.62). . . . .	59
12. Identified Mass Numbers in MMH/N <sub>2</sub> O <sub>4</sub> Exhaust. . . . .	61
REFERENCES . . . . .	64
NOMENCLATURE. . . . .	66

## 1.0 INTRODUCTION

There has been a continual need for a diagnostic technique that can be used to study chemical processes in the reacting flow fields of rocket engines. This need relates to such considerations as engine performance, radiation; gas dynamic interactions, and others. The parameters that most fully specify the chemical processes in flow fields as well as combustion chambers are species densities (mole fractions), total temperature, and the rotational and vibrational temperatures of the constituents. Various diagnostic techniques individually or collectively qualify as potentially useful tools for measurement of these parameters. However, since it has been suggested (Ref. 1) that minor constituents may play an important role in some of the observable effects relating to the characteristic performance of the total plume, an ultimately superior diagnostic technique for species density would be required to identify and measure species density with exceptional dynamic range. This requirement in particular makes mass spectrometry an attractive technique. Under sponsorship of the Defense Advanced Research Projects Agency (DARPA), the initial development of a mass spectrometry technique for the study of exhaust plumes of rocket engines was undertaken.

The initial objective of this experimental research effort was to explore and develop techniques and systems which offer promise in understanding certain properties of high altitude rocket plumes. In particular, the principal measurement capability desired by DARPA was the detection of unreacted minor hydrocarbon species in a rocket exhaust. The primary goals of this work were to design, construct, and test a mass spectrometer probe for farfield density measurements. The design criteria were to be compatible with tests to be conducted in the AEDC Aerospace Environmental Chamber (Mark I) of the von Kármán Gas Dynamics Facility. In particular, it was desired that meaningful plume measurements be made for a 75-lb-thrust, mono-methylhydrazine-nitrogen tetroxide rocket engine.

The designs considered during the conceptual phases of this activity had the benefit of previous experience of similar work performed in the AEDC Aerospace Chamber (10V) of the von Kármán Gas Dynamics Facility. The results of this earlier work, coupled with the potential Mark I utilization of the finished product, were most significant in determining the ultimate configuration. The high altitude and farfield constraints resulted from an attempt to avoid certain sampling and pumping problems that would certainly have existed with probe locations

too near the nozzle exit or with limited test chamber pumping speeds. The first requirement was that a container (probe) with internal pumping was necessary for providing a hard vacuum ( $10^{-7}$  torr) for the mass spectrometer head. Thus, the significant considerations were the determination of a method of pumping for the probe and a preferred sampling scheme to insure that the sample analyzed by the mass spectrometer was representative of the plume constituents.

Earlier 10V chamber work (Ref. 2) utilized a diffusion pump,  $\text{LN}_2$ , and LHe pumping media, the  $\text{LN}_2$  serving to pump high temperature ( $>77^\circ\text{K}$ ) condensables and as a shroud for the LHe pump. This had two serious disadvantages: (1) the probe was large, awkward, and required multiple utilities and (2) the additional difficulty of handling liquid helium. The latter was felt to be an important consideration for Mark I applications because of the large chamber size and the long transfer distance required if LHe were again used in a redesigned probe. It was thus determined that a preferable probe configuration would be one using GHe (or  $\text{LH}_2$  if desired) as a pumping medium with  $\text{CO}_2$  cryosorption pumping for the hydrogen present as a plume constituent. The following advantages are realized: (1) smaller probe size and cleaner design, (2) simpler and cheaper operation (no LHe required), and (3)  $\text{LH}_2$  may be used as an alternate cryogen.

## 2.0 PROBE DESIGN

In order to properly design a probe which will yield meaningful density measurements, one should know the rocket plume constituents, the performance characteristics of the rocket motor, the magnitude of probe effects, and the vacuum chamber performance during firing. Based on that knowledge, the size and positioning of a probe may be determined.

### 2.1 ROCKET PLUME CONSTITUENTS

The rocket engines to be used in the proposed plume tests utilize monomethylhydrazine (MMH),  $\text{NH}_2\text{NHCH}_3$ , as the fuel and nitrogen tetroxide,  $\text{N}_2\text{O}_4$ , as the oxidizer. The theoretical complete combustion composition of these propellants is given in Table 1. Since combustion is usually not complete, varying amounts of fuel (molecular weight = 46) and oxidizer (molecular weight = 92) may also be present. Approximately 16 percent of the exhaust is composed of hydrogen; thus, a suitable hydrogen pumping method must be incorporated into the probe

design. All other plume constituents are cryopumped at temperatures ranging from 77°K to 20°K.

**Table 1. Theoretical Plume Composition for Complete Combustion**

<u>Component</u>	<u>Mole Fraction</u>	<u>Molecular Weight</u>
H <sub>2</sub> O	0.3343	18
N <sub>2</sub>	0.3075	28
CO	0.1287	28
H <sub>2</sub>	0.1576	2
CO <sub>2</sub>	0.0401	44
OH	0.0111	17
H	0.0179	1
O <sub>2</sub>	0.0007	32
NO	0.0013	30
O	0.0008	16

## 2.2 PERFORMANCE CHARACTERISTICS FOR A 75-LB-THRUST ENGINE

The dimensions and operating characteristics for a 75-lb thrust MMH/N<sub>2</sub>O<sub>4</sub> engine tested in the Mark I vacuum chamber are given in Table 2. Impact pressure measurements at various locations downstream of the exit plane were taken during a rocket firing. The experimental results are recorded in Table 3.

The probe design was based on the 75-lb-thrust engine characteristics when operated in the Mark I chamber. The probe could then be employed in other chambers for sampling plumes of engines smaller in thrust than 75 lb.



**Table 2. 75-lb-Thrust Rocket Engine Characteristics**

Throat diameter	0.518 in.
Exit diameter	3.275 in.
Expansion ratio	40:1
Expansion type	Conical
Combustion chamber pressure	12,650 torr
Exit plane static pressure	19.65 torr
Stagnation temperature	~3,000°K
Vacuum chamber background pressure	$2.2 \times 10^{-2}$ torr

**Table 3. 75-lb-Thrust Engine Centerline Impact Pressure Measurements**

<u>X,</u> <u>in.</u>	<u><math>P_i/P_o</math></u>	<u><math>P_i</math>,</u> <u>torr</u>	<u>Mach Number,</u> <u><math>\gamma = 1.28</math></u>
24	$1.5 \times 10^{-3}$	19	8.45
36	$5 \times 10^{-4}$	6.3	10.02
48	$3 \times 10^{-4}$	3.8	10.8
60	$1.8 \times 10^{-4}$	2.3	11.7
72	$1.2 \times 10^{-4}$	1.52	12.4
84	$9 \times 10^{-5}$	1.14	12.96
96	$7 \times 10^{-5}$	0.89	13.4
108	$5 \times 10^{-5}$	0.63	14.1
120	$3.8 \times 10^{-5}$	0.48	14.7
132	$3.2 \times 10^{-5}$	0.40	15.08

X = Distance downstream from exit plane  
 $P_o$  = Stagnation chamber pressure  
 $P_i$  = Impact pressure

## 2.3 MASS-SAMPLING CONSIDERATIONS

Prior to establishing exact dimensions and characteristics of the mass spectrometer probe, several problem areas had to be investigated. The insertion of a probe into a flow field necessarily generates interactions between the probe and flow. For proper sampling, these interactions must either be eliminated or compensated for during data reduction. The interactions may affect the mass spectrometer measurements in two specific ways, the probe may induce changes in relative and absolute species number densities and/or in the species velocity distributions. Unfortunately, calibrations cannot successfully recover exact number density or velocity distribution data from measurements affected by probe flow-field interactions. It is thus desirable to at least minimize, if not eliminate, the interactions in question.

The two skimming systems capable of reducing interaction effects are a cryogenically pumping skimmer and a slender nonpumping skimmer. Both systems were examined for their applicability to specific situations.

### 2.3.1 Shock-Induced Mass Separation

A large number of experimental investigations designed to measure mass separation effects in high-speed flow fields have been carried out. In many cases, mass-sampling probes were inserted into the flow and the captured gas analyzed to determine the relative species concentrations. In a large percentage of the experiments, the separation effects of the probe resulted in completely masking the flow-field separation effects. In an early experiment for example, Chow (Ref. 3) reported that in the diffusive separation of binary mixtures in free jets, the heavy specie was predominant in all regions of the jet. The proper conclusion was that the sampling probe Chow employed produced strong velocity gradients (shocks) at the probe entrance. The light specie, nitrogen, was more capable of following these strong gradients around the probe than the heavy specie, oxygen. Hence, the heavy specie was always predominant inside Chow's sampling probe. More current experiments, such as the ones by Rothe (Ref. 4) for helium and argon mixtures, have demonstrated the effect of normal shocks on mass separation by employing electron beam probing of the flow inside a shock holder. These experiments dramatically demonstrate the light specie depletion.

Due to these considerations, the elimination of a normal shock at the probe sampling orifice must be achieved in order to insure a proper representation of plume constituents. Since the probe is to sample in

the farfield, the concept of a thin normal shock at the skimmer is inapplicable. Nevertheless, the gradients introduced for even thick shock systems are sufficient to bias the probe with regard to the very light species of interest such as hydrogen and the light hydrocarbons.

### **2.3.2 Velocity Distribution Alteration due to Shock Waves**

The time-of-flight velocity technique (Ref. 5) may be employed with a mass spectrometer type probe to obtain the velocity distribution of the molecules entering the probe. From the velocity distribution it is possible to obtain the flow parallel static temperature component, and in the case of cold flow, to determine plume stagnation temperatures. Combustion chamber temperature measurements are not feasible because of the nonequilibrium flow present in a rocket motor.

If shocks exist at the skimmer entrance to the probe, the temperatures are raised upon crossing these shocks and no reliable measure of static gas temperature can be obtained.

### **2.3.3 Internal Mass Separation**

The principle on which the mass spectrometer probe is based is that it performs as a molecular beam system. The probe maintains a very low internal pressure while immersed in a plume. The probe-sampling orifice skims off a portion of the plume and forms an internal molecular beam. When a multispecied molecular beam is formed, the beam species are known to spread at different rates because of the differences in their molecular weights. Stephenson (Ref. 6) has taken advantage of this effect in the use of heated hydrogen-argon expansions to produce very high energy argon beams.

The amount of separation of the light specie in the probe for a binary mixture molecular beam is proportional to the distance from the skimmer to the ion source and inversely proportional to the square root of the species molecular weight. Since the distance is the only adjustable probe parameter, it should be kept at the minimum practical length.

### **2.3.4 External Scattering in Rarefied Flow**

Skimmer effects upon molecular beam parameters are a major consideration in any molecular beam experiment. In the case of constituency measurements, unless the species are condensed, the skimming process is a problem only when a shock is formed at the skimmer or when

sampling very rarefied regions where the splashing of molecules from the skimmer significantly deteriorates the molecular beam. The effects of shocks were discussed previously in this report. For the noncondensed case, as in most portions of a rocket plume, there are two solutions to the external backscatter problem. One is to have a pumping skimmer which allows very little backscatter. This would be applicable to continuum as well as rarefied flows but is not always feasible because of its inability to pump all species well or to handle excessive heat loads. The second is to calibrate the probe system by using flows of well documented, easily varied, number density. This allows the signal degradation due to backscatter to be compensated during data analysis. In either event, this must be considered during skimmer design.

### 2.3.5 Internal Scattering

Once the molecular beam is formed inside the probe, scattering between the beam molecules and the probe background molecules must be considered. Previous experiments have shown that once the probe background number density reaches a given level the beam is degraded significantly. This, coupled with the ordinary signal-to-background molecule noise in the mass spectrometer, makes proper interpretation of mass spectrometer signals very difficult. It has been shown in a prior investigation (Ref. 2) that this problem can be completely neglected if the probe pressure (equivalent to a beam test chamber pressure) is maintained in the  $10^{-7}$  torr range.

## 2.4 PROBE SIZING AND POSITIONING

With regard to the optimum physical size of the probe and its position in the rocket plume, several criteria should be met. If possible the probe should be (1) located in a rarefied region of the flow field, i. e., where the Knudsen number ( $K_n$ ) based on skimmer diameter is greater than one; this location should create only a small flow disturbance and also would avoid any reexpansion of the plume sample after skimming, (2) able to internally pump the hydrogen gas load entering the skimmer, and (3) located upstream of the plume Mach disk. In an attempt to adhere to these criteria, the following calculations were made. The Knudsen number is given as

$$K_n = \lambda / D_{SK}$$

where  $\lambda$  is the mean free path at the skimmer and  $D_{SK}$  is the diameter of the skimmer. For the expansion of a jet into a vacuum, Bossel (Ref. 7) gives the following relations for the mean free path:

$$\lambda/\lambda_o = \left(1 + \frac{\gamma-1}{2} M^2\right)^{\frac{\gamma-1}{2(\gamma-1)} - \omega} \quad (1)$$

where  $\lambda_o$  is the combustion chamber mean free path

$\omega$  is the exponent in the viscosity-temperature relation

$\gamma$  is the specific heat ratio

$M$  is the Mach number

He also found that for large values of the ratio of downstream distance to nozzle exit diameter ( $X/D_e$ ),

$$\lambda/\lambda_o = \text{const } (X/D_e)^2 [1 - (\gamma-1)(\omega-0.5)] \quad (2)$$

If it is assumed that  $\omega = 0.5$  for the rocket plume, then the constant in Eq. (2) may be evaluated by equating Eqs. (1) and (2) and utilizing the experimental data. The following approximation for the mean free path results:

$$\lambda \approx 3.91 \lambda_o (X/D_e)^2$$

Since the plume consists of a mixture of gases,  $\lambda_o$  must be estimated. The combustion chamber mean free path is related to a reference mean free path at standard conditions by the following relation:

$$\lambda_o = \lambda_{ref} (P_{ref}/P_o) (T_o/T_{ref})$$

where  $P_{ref} = 760$  torr

$P_o = 12,650$  torr

$T_{ref} = 293^\circ\text{K}$

$T_o = 3,000^\circ\text{K}$

The mean molecular weight of the combustion products is approximately 18 gm/mole. An examination of the mean free paths of various gases over a range of molecular weights indicated that an assumed value of  $\lambda_{ref} = 10^{-5}$  cm would be reasonable at standard conditions. Therefore, with this assumption and the previous reference values, one obtains

$$\lambda_o = 6 \times 10^{-6} \text{ cm}$$

The expression for the mean free path as a function of  $X/D_e$  becomes

$$\lambda = 2.34 \times 10^{-5} (X/D_e)^2$$

Therefore, to insure free molecular flow, the probe size and positioning should satisfy the following criterion:

$$K_n = \frac{\lambda}{D_{SK}} = \frac{2.34 \times 10^{-5} (X/D_e)^2}{D_{SK}} > 1$$

In order to make reliable mass spectrometer measurements, the internal probe pressure should be maintained in the low  $10^{-7}$  torr range. To provide the necessary pumping speed and capacity, cryosorption pumping (Ref. 8) at frost temperatures less than  $20^\circ\text{K}$  may be utilized. All plume gases with the exception of hydrogen are readily pumped on these cryosurfaces, provided, of course, that the refrigeration capacity of the pumping system is not exceeded. Thus, attention must be focused on the hydrogen pumping requirements. Consider the following equality:

$$A_{\text{pump}} \times S_1 \times P_p = \text{Thruput}$$

where  $A_{\text{pump}}$  is the internal probe pumping area  
 $S_1$  is the hydrogen pumping speed (e.g.,  $S_1 \approx 30 \text{ l/sec cm}^2$  using  $\text{CO}_2$  as the cryosorbent at  $12^\circ\text{K}$ , Ref. 8)  
 $P_p$  is the desired internal probe pressure ( $\sim 10^{-7}$  torr)

The thruput is given by:

$$\text{Thruput} = \dot{m}RT = P_s A_{SK} M_{SK} \sqrt{\gamma RT_s}$$

where  $P_s$  is the static pressure at the skimmer  
 $A_{SK}$  is the cross-sectional area of the skimmer  
 $M_{SK}$  is the local Mach number at the skimmer  
 $R$  is the gas constant.

The Mach number at a given centerline position may be estimated from the available experimental data (Table 3) and the other flow quantities (which are functions of the Mach number) can be found from the appropriate gas tables. Thus, the location of the probe in the plume and the dimensions should satisfy the following relation:

$$A_{\text{pump}} \times S_1 \times P_p = P_s A_{\text{SK}} M_{\text{SK}} \sqrt{\gamma R T_s}$$

In order to avoid additional potential difficulties in obtaining a plume sample, the probe must be located upstream of the plume Mach disk. The Mach disk location is given as (Ref. 9)

$$X_{M_d}/r_e = 1.38 M_e \sqrt{\gamma P_e/P_\infty} \quad (3)$$

where  $X_{M_d}$  is the axial distance from the nozzle exit plane to the Mach disk  
 $r_e$  is the nozzle exit radius  
 $P_e$  is the exit static pressure  
 $P_\infty$  is the vacuum chamber static pressure.

When the 75-lb-thrust engine is fired in the Mark I chamber, the Mach disk is located at:

$$X_{M_d} \approx 360.6 \text{ in.} = 30.1 \text{ ft}$$

These three criteria were utilized in determining the size and prospective positioning of the probe. Using trial and error, the following design parameters and flow conditions of Table 4 were selected.

**Table 4. Design Parameters and Flow Conditions**

Skimmer diameter, $D_{\text{SK}}$	2 mm
Internal probe area, $A_{\text{pump}}$	1,125 cm <sup>2</sup>
Probe location, X	11 ft = 335 cm
Knudsen number, $K_n$	7.6
Mach number, $M_{\text{SK}}$	15
Static temperature, $T_s$	100°K
Static pressure, $P_s$	$2 \times 10^{-3}$ torr
Impact pressure, $P_i$	0.4 torr

Although design criteria have been determined, the actual performance of the probe can only be found by experimentation. This is due to the uncertainty in the expansion characteristics and interactions of high enthalpy plume gases with cryogenically cooled surfaces and the operating characteristics of system electronics. Therefore, two probe designs were proposed: (1) a "flat-face" cryogenic skimmer probe (Fig. 1) and (2) a conical, warm skimmer probe (Fig. 2). The designs contained the following features:

1. The probe chamber assembly consists of two parts:
  - (a) Stainless steel concentric cylinders ("flat-face" probe) or cones (conical probe) in which gaseous helium is circulated. This probe section serves not only as the internal but also as an external pump.
  - (b) An uncooled cylindrical stainless steel shell on which the mass spectrometer and an ion gage are mounted. This section is compatible with either the cylindrical or conical cooled sections of (a).  
The two sections are joined by stainless steel flanges separated by a Kel-F<sup>®</sup> gasket. The design allows easy access to the electronic components as well as preventing sublimation of pumped plume gases from intermediate temperature surfaces.
2. Each probe has a carbon dioxide injector tube which is utilized in CO<sub>2</sub> addition for cryosorption pumping of hydrogen.
3. Each probe contains an EAI quadrupole mass spectrometer with an offset electron multiplier and an ion gage for internal background pressure monitoring.
4. The two probe geometries have their own unique advantages and disadvantages:
  - (a) The "flat-face" design allows the mass spectrometer ionization section to be positioned very near the skimmer entrance and thus minimizes alignment error, beam scattering, and internal mass separation. The usefulness of this probe will be limited by pumping breakdown on the flat-face in the presence of excessive external heat loads. This limit must be determined experimentally.



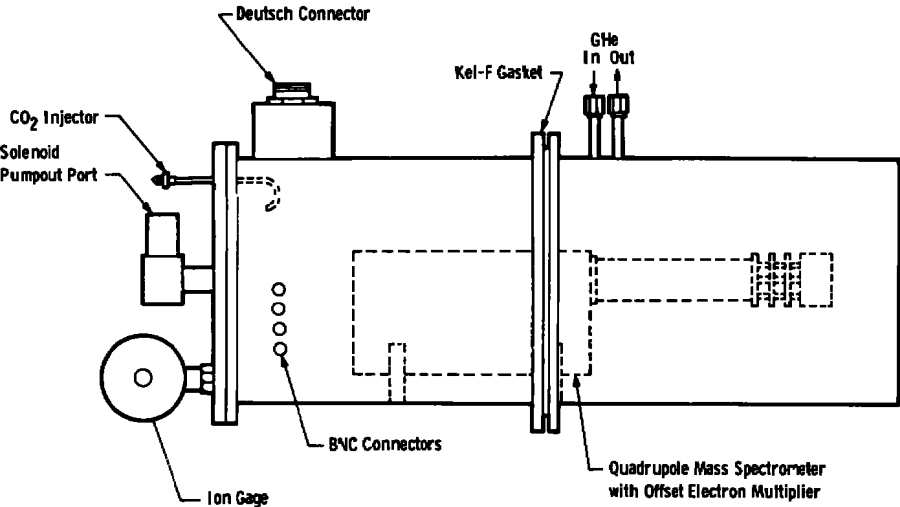


Figure 1. Schematic of flat-face probe.

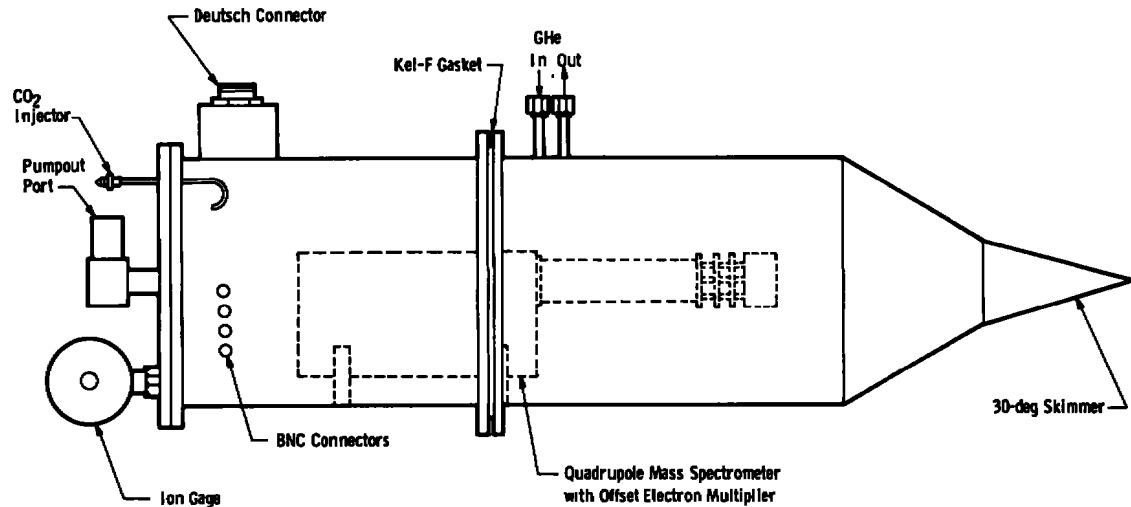


Figure 2. Schematic of conical probe.

- (b) The conical face probe would tend to reduce the external scattering in regions of high impact pressure. The 30-deg, thin-walled skimmer tip was fabricated by electroplating nickel onto an aluminum pattern and then dissolving the aluminum in a sodium hydroxide solution. The skimmer was then soldered to the stainless steel conical section. This configuration had the possible disadvantage of having intermediate temperature surfaces near the skimmer tip which could interfere with internal sample collection because of scattering, hence a skimmer heater was added.

One of the goals of this research was to experimentally compare the operational characteristics of these two probes. Section 3.0 will discuss the methodology and procedures used in the comparison, and Section 4.0 will present the experimental results for free-jet sampling of cold flows (300°K).

## 2.5 INSTRUMENTATION DESIGN CONSIDERATIONS

The instrumentation systems of interest were those dealing with the mass spectrometer head and probe support instrumentation.

The mass spectrometer was a commercial version of the quadrupole. Standard quadrupole electronic packages were thus used, consisting of ion source and power supplies and emission controllers, quadrupole and power supply (RF/DC), and particle multiplier and high voltage power supply. Because of the anticipated sweep rates and the TOF velocity measurement, signal amplification from the particle multiplier was required. For frequency response purposes and high gain requirements a large multiplier load resistor and preamplifier had to be physically located at the last dynode. An FET input operational amplifier with a gain of ten was used for this application and located within the vacuum system.

The metastable velocity measurement application required pulsing the electron grid. This was implemented by placing in series, between power supply and the grid, the secondary of a pulse transformer. The power supply voltage was placed slightly below threshold and pulsed with a Rutherford® pulse generator across the transformer primary. The length of the filter section plus the separation of the quadrupole and multiplier apertures was taken as the flight distance. The preamplifier mentioned above, with a band width in excess of 1 MHz would be adequate for density or velocity measurements.

Supporting instrumentation consisted of probe temperature and pressure-measuring systems. Conventional thermocouples were used down to cryogenic temperatures. In the cryogenic range ( $< 30^{\circ}\text{K}$ ), thermistors mounted in copper blocks through which the system cryogen passed were used in both input and return coolant lines. Calibrations were required for these devices.

A General Electric Ion Gage was used for probe pressure measurements. This selection provided for pressure measurements from 100  $\mu\text{Hg}$  and lower. In addition, utilization of these gages provided a mechanism for mass spectrometer automatic shutdown in the case of excessive probe pressures. The gage was physically located in the aft end of the probe, i. e., the warm section, and thus gave a worst case pressure reading since the principle part of the head assembly was located in the cryogenic section and experienced a lower than indicated pressure.

### 3.0 EXPERIMENTAL PROCEDURE

The experimental cold flow testing of the conical and "flat-face" probes was conducted in the Aerodynamic Molecular Beam Chamber (Fig. 3) and the 4- by 10-ft Research Chamber (Fig. 4). The operational characteristics and pumping capabilities of these chambers have been discussed in detail elsewhere (Refs. 10 and 11). Suitable probe mounting devices were designed and built for both test cells. An experimental plan consisting of six steps was initiated:

- Step 1: Evaluate the hydrogen sorption pumping capability of carbon dioxide in the probe.
- Step 2: Evaluate system response for a plume sample using (a) an easily pumped gas (e. g.,  $\text{N}_2$  or Ar) and (b) a hydrogen mixture.
- Step 3: Evaluate probe performance for various impact pressures and/or heat loads.
- Step 4: Evaluate the interference to plume sampling by the invasion of background gas both internal and external to the probe.
- Step 5: Determine each probe's operational ranges and limits.
- Step 6: Based on cold flow experiments, design a new probe for actual testing in a rocket exhaust plume.

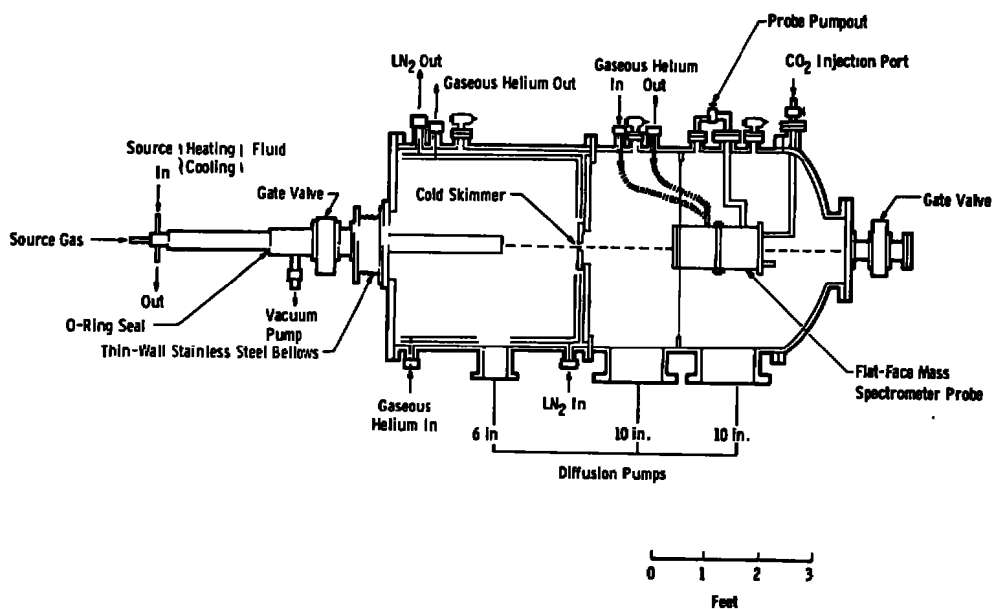


Figure 3. Schematic of the molecular beam chamber.

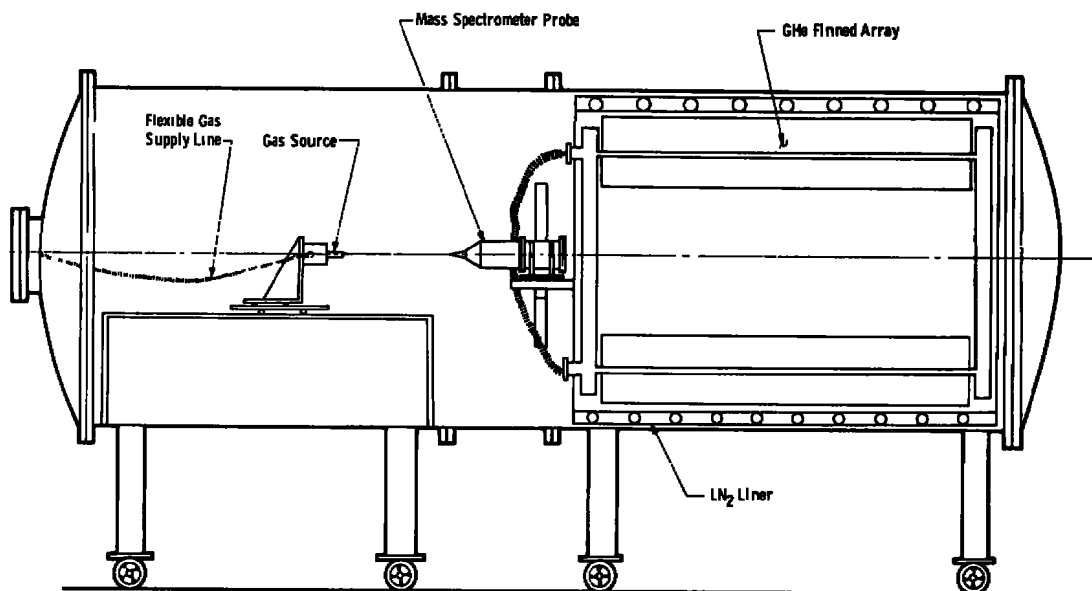


Figure 4. Schematic of 4- by 10-ft research vacuum chamber.

For an experimental test run the basic procedure was as follows:

1. The vacuum chamber and probe were evacuated with mechanical and diffusion pumps.
2. The chamber and probe were cooled down simultaneously with gaseous helium. The GHe flow rate through the probe could be varied with a cryogenic throttling valve.
3. The carbon dioxide cryosorbent was slowly deposited internally to the probe, e. g.,  $P_{\text{CO}_2} \approx 10^{-4}$  torr, for approximately five minutes.
4. If liquid helium pumping were unavailable, then carbon dioxide was slowly deposited on the external gaseous helium surfaces at rates similar to that given in No. 3.
5. The mass spectrometer with its associated electronics and the remaining chamber instrumentation were activated.
6. The particular experiment of interest was then performed.

## 4.0 PROBE PERFORMANCE IN COLD FLOWS

### 4.1 FLAT-FACE PROBE

The initial testing of the "flat-face" probe was carried out in the Aerodynamic Molecular Beam Chamber. Steps 1 through 5 of Section 3.0 were performed in that chamber.

#### 4.1.1 Probe-Pumping Evaluation

An experimental evaluation of the probe pumping, including carbon dioxide cryosorption, was made. The results are summarized in Figs. 5 through 7. Figures 5 and 6 represent data obtained by bleeding hydrogen into the vacuum chamber background. For the case presented in Fig. 5, no  $\text{CO}_2$  was predeposited. When hydrogen was introduced into the background, the probe internal pressure was identical to the chamber pressure. However, after the internal predeposition of  $\text{CO}_2$  for five minutes at a probe pressure of  $10^{-4}$  torr, the results were radically different (Fig. 6). As the vacuum chamber approached  $10^{-4}$  torr of hydrogen, the probe pressure remained unchanged at  $10^{-7}$  torr. The results of these experiments confirmed the necessity of cryosorption pumping for testing of gases with significant hydrogen content.

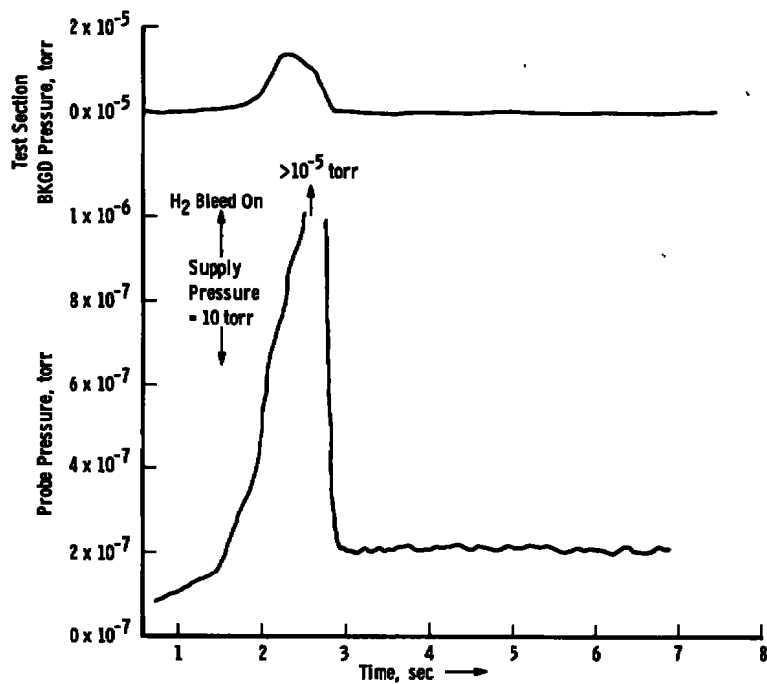


Figure 5. Probe pressure response for no CO<sub>2</sub> deposition.

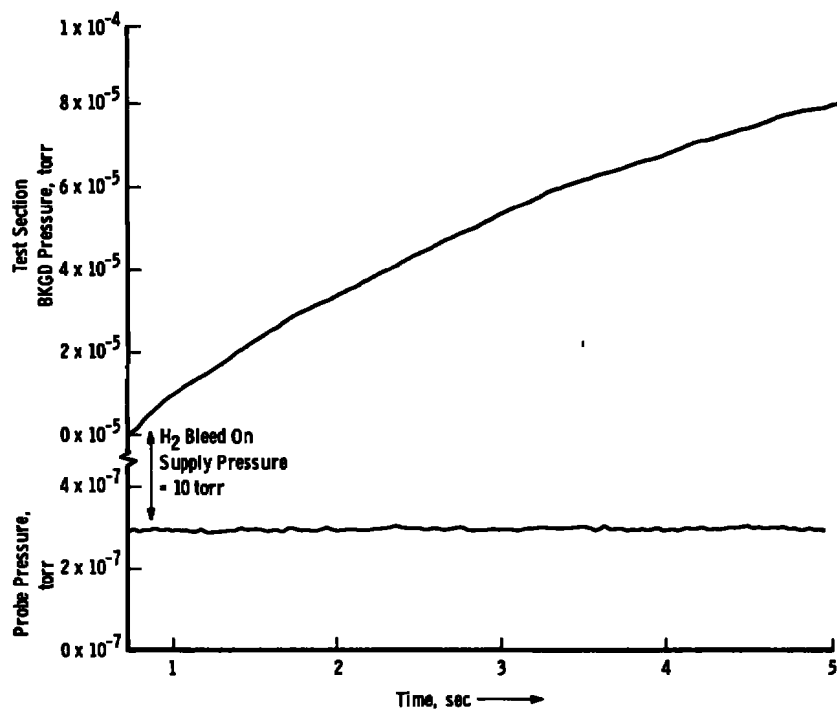


Figure 6. Probe pressure response for CO<sub>2</sub> deposition.

The typical pumping performance of the flat-face probe during free-jet sampling of several source gases is presented in Fig. 7. The internal probe pressure behavior is presented as a function of impact pressure at the skimmer entrance. The probe-pumping system is seen to perform well (remaining on the  $10^{-7}$  torr scale) for the pure gases but deviates significantly for the hydrogen mixture.

#### 4.1.2 Plume-Sampling Measurements

Probe performance measurements were initially made for easily pumped gases, i. e., nitrogen and argon. Typical results are presented in Figs. 8 and 9 along with the corresponding values of test chamber and internal probe pressure. The variation of mass spectrometer signal for increases in source stagnation pressure is basically linear until condensation of the test gas occurs at large stagnation pressures (Ref. 12). These results indicate that the probe functioned satisfactorily for these particular source conditions and separation distances.

Having established the probe's ability to sample easily pumped gases, hydrogen mixtures were tested. Typical results for a simulated rocket plume (51-percent  $N_2$ , 27-percent  $H_2$  and 22-percent  $CO$ ) are shown in Fig. 10 for various nozzle-probe separations. A decided improvement was demonstrated for the performance when  $CO_2$  was deposited on the front face. The maxima seen in each curve can be attributed to pumping breakdown on the front face. Mach disk interference can be ruled out since, although it does contribute for the cases without  $CO_2$  addition, it does not occur for the other case and the same behavior is demonstrated.

In an effort to simulate a minor specie plume component, a 1-percent concentration of argon was added to a similar gas mixture, i. e., 27-percent  $H_2$ , 51-percent  $N_2$ , 21-percent  $CO$  and 1-percent  $Ar$ . Some results are shown in Fig. 11. The argon signal was monitored as the stagnation pressure was increased, and once again a breakdown in the curve was observed. Apparently, at this point the incident gas load exceeds the pumping capacity of the probe.

One additional mixture (20-percent  $H_2$ , 80-percent  $CO_2$ ) was investigated. Typical results are presented in Fig. 12. Once again, the probe performance was linear until pumping breakdown occurred.

#### 4.1.3 Calculation of Impact Pressures at Pumping Breakdown

The impact pressures which correspond to the maxima of the probe performance curves of Section 4.1.2 may be calculated using the relation of Sherman and Ashkenas (Ref. 13), i. e.,

$$P_i = P_o \left( \frac{\gamma+1}{\gamma-1} \right)^{\frac{\gamma}{\gamma-1}} \left( \frac{\gamma+1}{2\gamma} \right)^{\frac{1}{\gamma-1}} A^{\frac{-2}{\gamma-1}} \left( \frac{X-X_o'}{D} \right)^{-2}$$

where  $P_i$  is the impact pressure,  
 $P_o$  is the stagnation pressure,  
 $\gamma$  is the ratio of specific heats,  
 $A$  is a constant ( $= 3.65$  for  $\gamma = 1.4$ ) ( $= 3.96$  for  $\gamma = 1.2857$ ),  
 $X$  is the nozzle-skimmer separation distance,  
 $D$  is the nozzle diameter, and  
 $X_o'$  is the distance to a virtual "source" but is negligible for these calculations.

For the curves of Figs. 10 and 11 the relation reduces to

$$P_i/P_o \approx 0.556 (X/D)^{-2} \quad (\gamma = 1.4)$$

and for Fig. 12,

$$P_i/P_o \approx 0.523 (X/D)^{-2} \quad (\gamma = 1.28)$$

Thus, the impact pressure at pumping breakdown in Fig. 10 at  $X = 10$  in. and a  $\text{CO}_2$  frost externally deposited is  $1 \times 10^{-4}$  torr. For Figs. 11 and 12 the impact pressures are  $8.23 \times 10^{-4}$  torr and  $2.86 \times 10^{-3}$  torr, respectively. Unfortunately, these impact pressures for which an undisturbed sample may be taken are nearly two orders of magnitude lower than that to be encountered during the rocket firing if the probe is positioned 11 ft from the 75-lb-thrust rocket exit plane. However, if a 1-lb-thrust engine is used ( $P_o = 90$  psi,  $D_{\text{Throat}} = 0.09$  in.), the probe could be positioned at 10.2 ft and be within the range of undisturbed sampling.

## 4.2 CONICAL-FACE PROBE

The performance testing of the conical skimmer probe was conducted in the 4- by 10-ft Research Vacuum Chamber. The same experimental procedure that was outlined for the flat-face probe was employed in evaluating the conical probe performance.



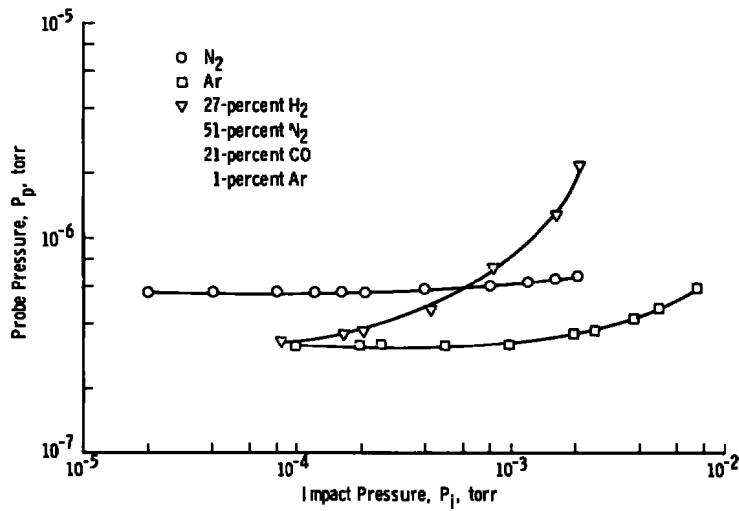


Figure 7. Probe pressure versus impact pressure.

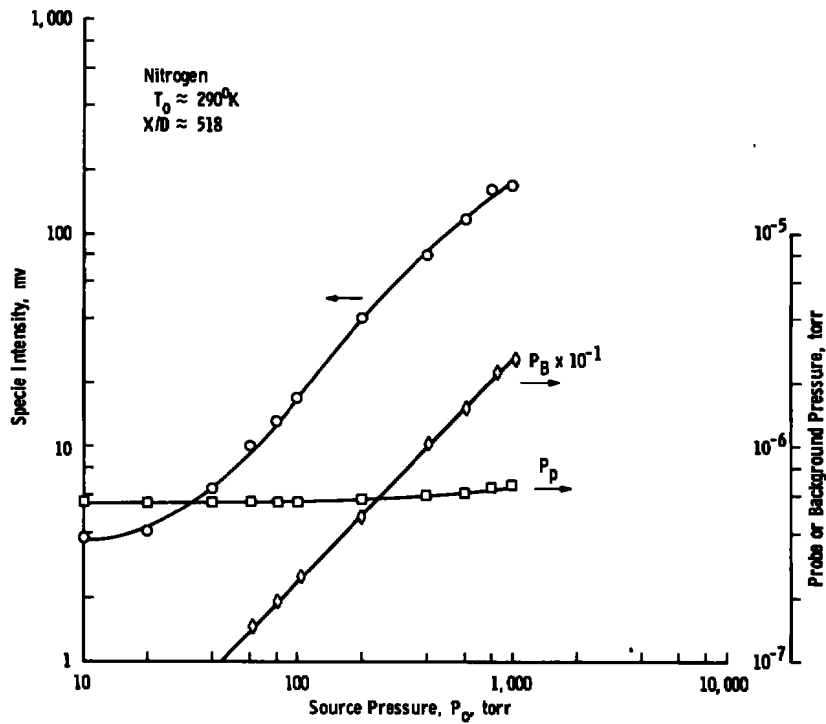


Figure 8. Flat-face probe performance for nitrogen.

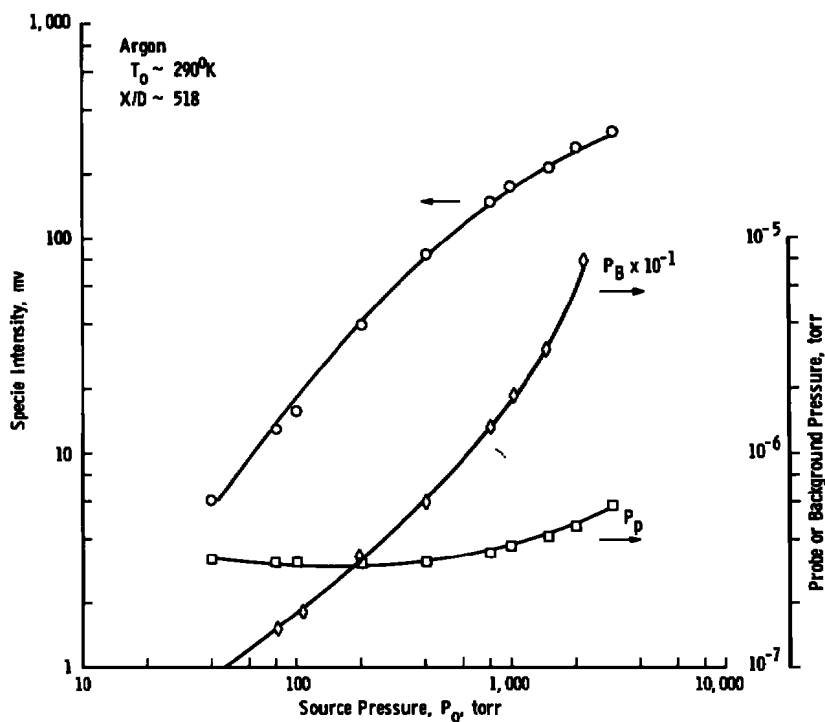
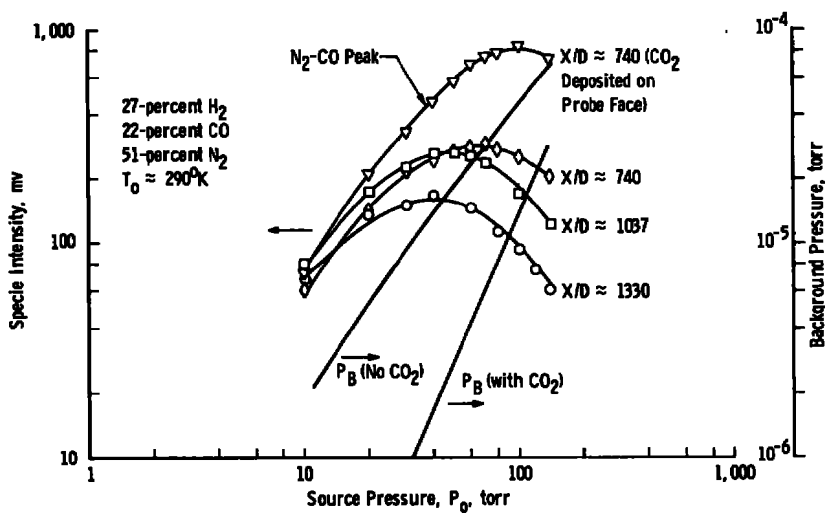


Figure 9. Flat-face probe performance for argon.

Figure 10. Flat-face probe performance for  $\text{H}_2$ ,  $\text{CO}$ ,  $\text{N}_2$  mixture.

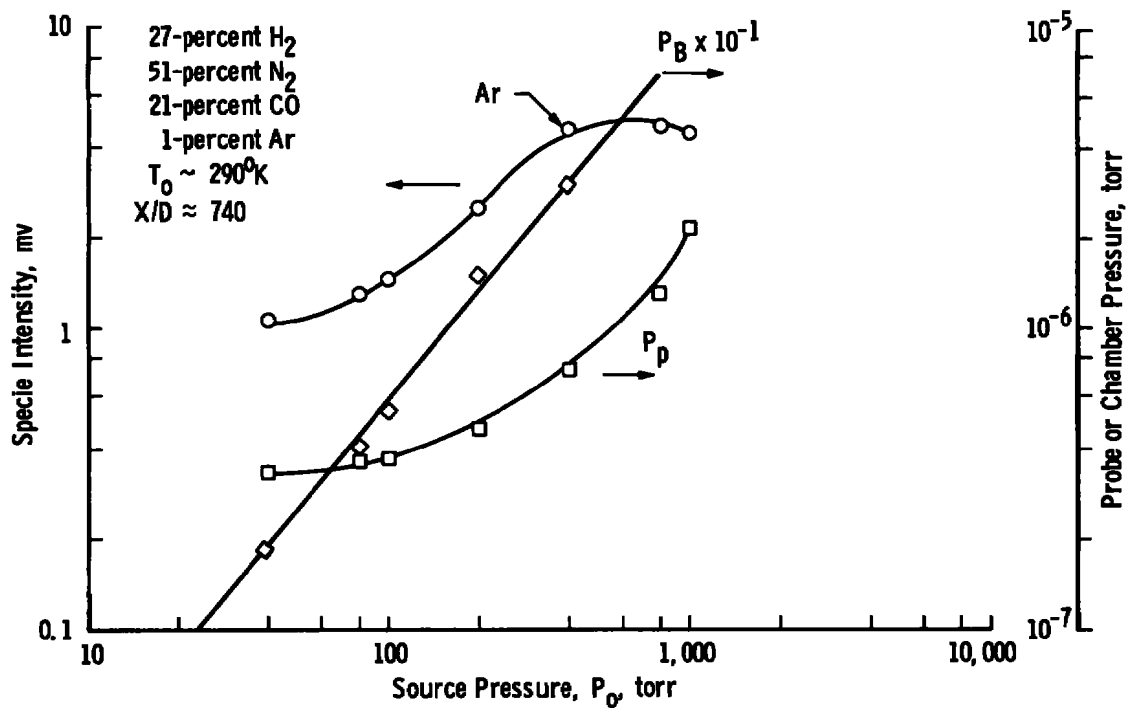


Figure 11. Minor species measurement.

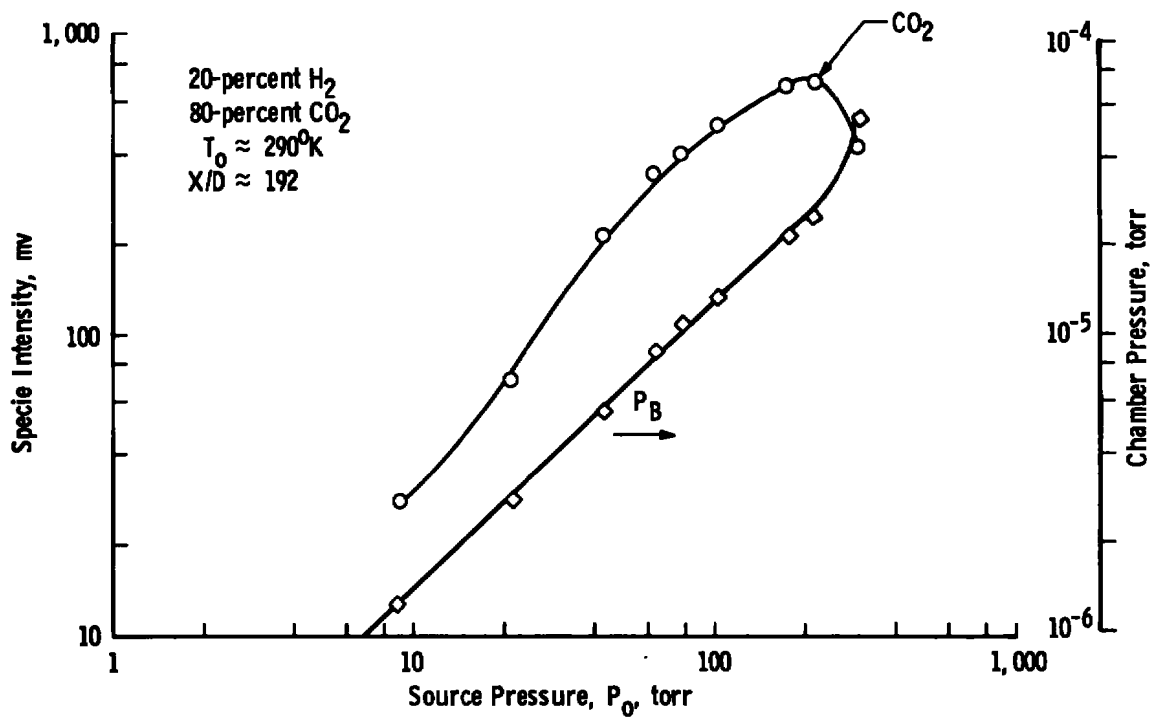


Figure 12. Flat-face probe performance for hydrogen and carbon dioxide.

### 4.2.1 Probe-Pumping Evaluation

The internal pumping system for the two probes differs due to the shape of the systems only. Since the conical-faced probe has more internal surface area, it was expected to possess a higher pumping speed.

Figure 13 presents representative pumping data for the conical probe for pure nitrogen and several  $H_2$ ,  $CO_2$  mixtures. The curves presented for the hydrogen mixtures when no  $CO_2$  was predeposited would demonstrate the lower degree of pumping even more drastically except that the  $CO_2$  in the mixtures gave a self-pumping character to the gas. The lower values of probe pressure for a given impact pressure indicate the conical-face probe's superior pumping ability. The impact pressure is a good indicator of the mass flux into the probe and since it is easily calculated or measured (Ref. 13), it is the coordinate choice for presentation of the pumping data.

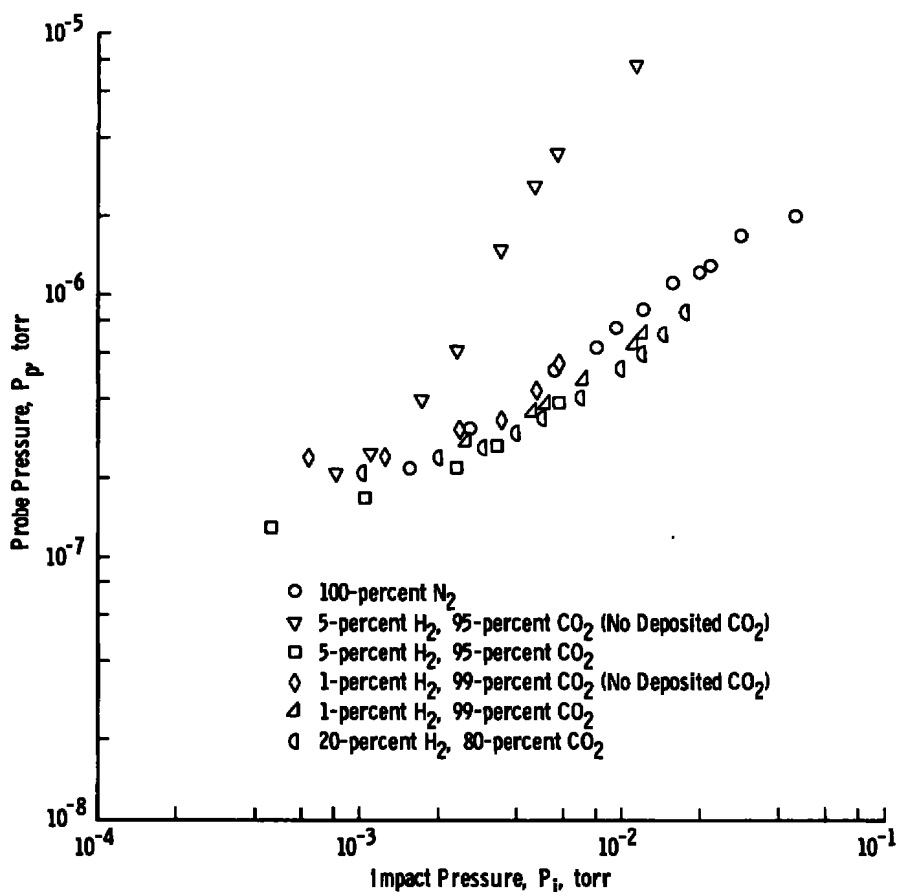


Figure 13. Conical probe pumping performance.

#### 4.2.2 Plume-Sampling Measurements

Following the same general approach taken for the flat-face probe, the sampling ability of the conical probe was initially investigated for more easily pumped gases. Typical results for nitrogen are presented in Figs. 14 and 15. The difference in magnitudes of the mass spectrometer output signals in the two figures is related to variation in mass spectrometer settings and sensitivity shifts. When quantitative measurements are to be made, the mass spectrometer must be calibrated immediately prior to the day's experiment to compensate for this problem. The data for the two figures are seen to possess good qualitative agreement.

Representative results for sampling mixtures containing hydrogen are demonstrated in Figs. 16 and 17. The data for the 1-percent  $H_2$ , 99-percent  $CO_2$  demonstrate the ability to monitor a minor specie which is not well suited to mass spectrometer detection. In general, the detection of small hydrogen peaks is very difficult and requires maximum sensitivity of the quadrupole. Ability to detect such a small quantity of  $H_2$  and retain the  $CO_2$  peak resolution reaffirmed the probe's applicability for minor specie sampling of a rocket exhaust plume.

#### 4.2.3 Impact Pressures at Pumping Breakdown

The impact pressure at which "pumping breakdown" occurs varies from one data set to the other. The variation of the breakdown pressure was influenced by the changes in the amount of coolant flow, the variation of the  $CO_2$  frost (regardless of how carefully deposited), chamber background pressure, and others. Although in principle none of these except the coolant flow should be significant, the combined contribution of such parameters is impossible to predict. It is felt that the coolant flow rate was the primary concern. A small change in the gaseous helium flow to the probe can produce a significant gradient across the  $CO_2$  sorbent. This can affect the hydrogen pumping which could lead to "pumping breakdown," in reality a possible misnomer since internal scattering could be the cause. The exact precipitator of the pumping breakdown for the conical probe is undeterminable at present.

The impact pressures at breakdown were approximately  $3.5 \times 10^{-2}$  torr for nitrogen and  $1.35 \times 10^{-2}$  torr for the hydrogen mixtures. These impact pressures are as much as two orders of magnitude greater than those tolerated by the flat-face configuration. Hence, the conical probe is capable of sampling in a higher impact pressure environment than is the flat-face probe. This was to be expected since warm conical skimmers are generally chosen for sampling high-pressure flow fields.

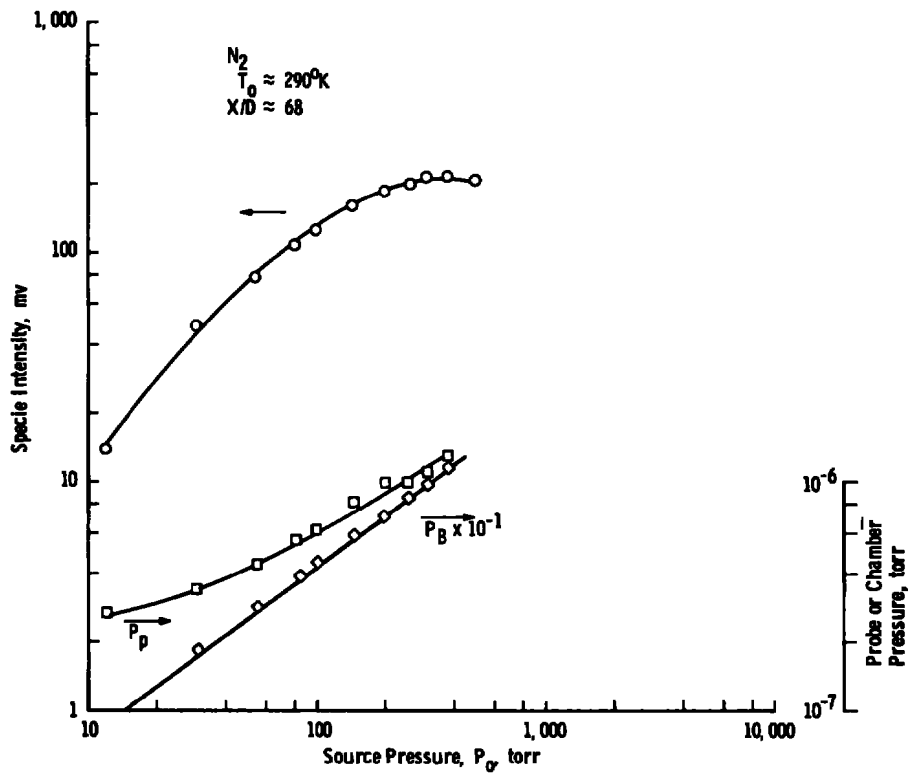
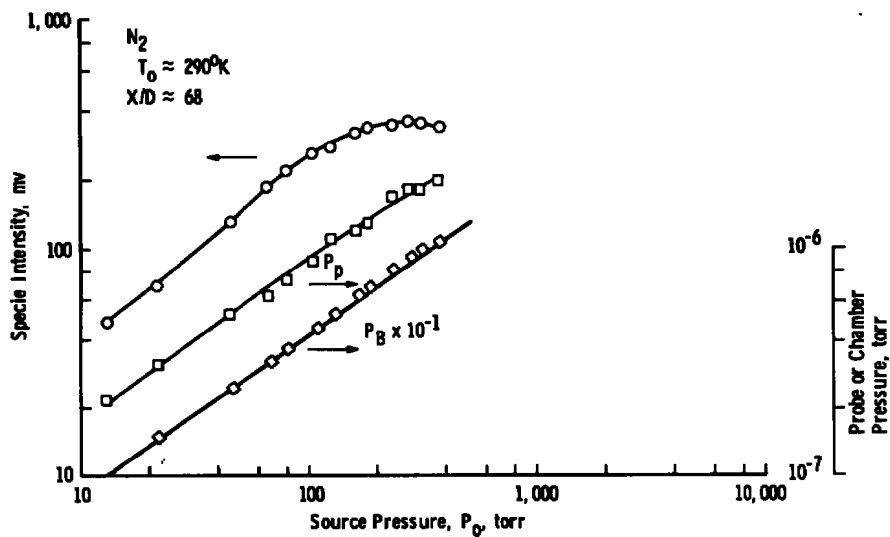


Figure 14. Conical probe performance for nitrogen.

Figure 15.  $N_2$  performance for the conical probe.

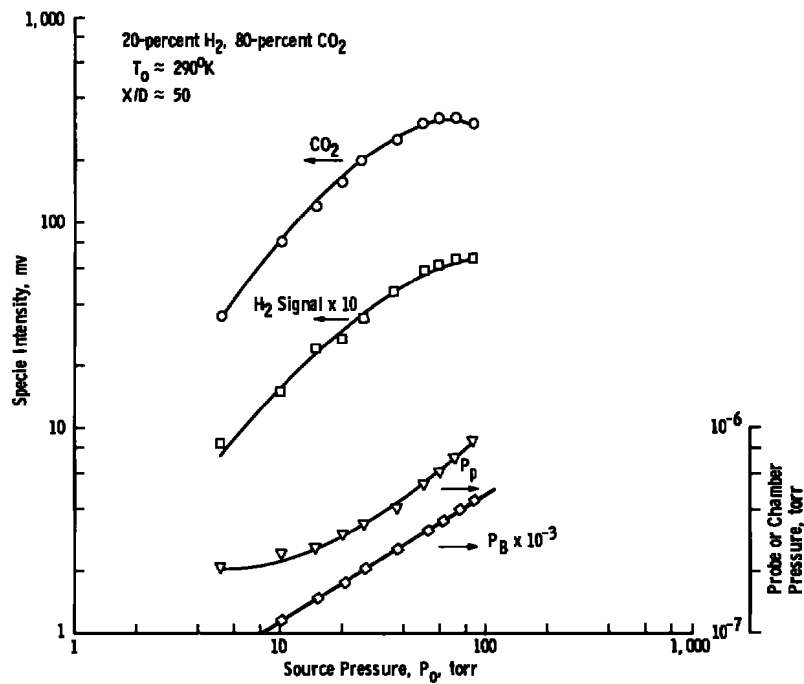


Figure 16. Conical-face probe performance in a 20-percent  $H_2$ , 80-percent  $CO_2$  jet.

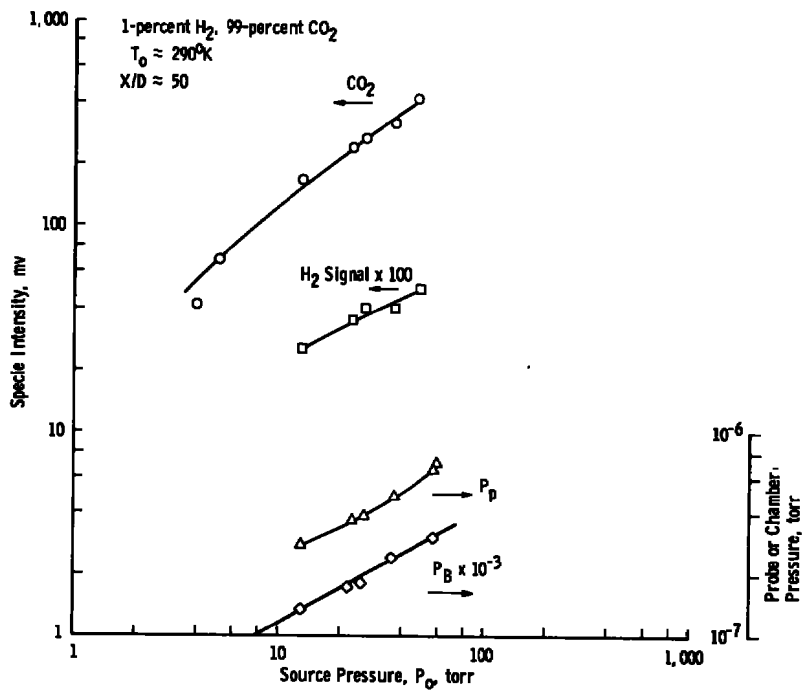


Figure 17. Conical probe performance in a 1-percent  $H_2$ , 99-percent  $CO_2$  mixture.

In the 75-lb-thrust rocket engine plume the conical probe would be incapable of handling the impact pressure at 11.2 ft. However, at a location just inside the Mach disk the conical probe could possibly sample and measure properly the constituency of the 75-lb-thrust engine plume. For smaller engines, the conical probe would definitely be capable of mass sampling the plume.

#### 4.3 MASS SPECTROMETER PERFORMANCE

The mass spectrometer system employed in both the probes included an EAI® pole section, an RF power supply and associated electronics, an Extranuclear Laboratories® ionizer assembly with its associated electronics, and an Extranuclear Laboratories paraxial electron multiplier system with a high voltage supply. A photograph of the mass spectrometer assembly, its mount, and the two probes is presented as Fig. 18.

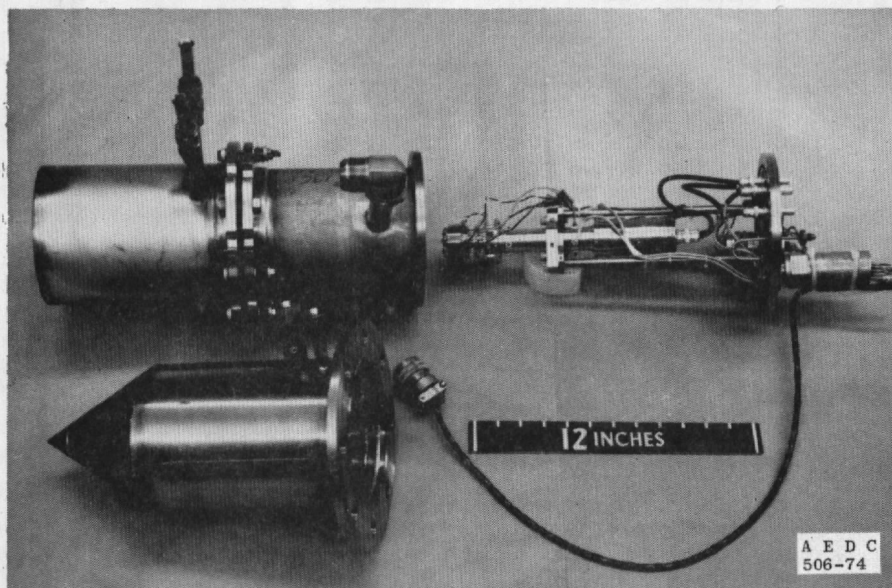


Figure 18. Mass spectrometer, probe and assembly.

##### 4.3.1 Ionizer for Mass Filter Assembly

The axial ionizer is designed specifically for ionizing molecular beams. The beam enters on the geometrical axis of the ionizer and quadrupole as shown in Fig. 19. While in the ionizing region, the beam passes along the axis of a cylindrical grid which accelerates electrons towards the axis from four filaments which form a square surrounding the grid. Extremely high emission currents are possible from such an arrangement. The ions



are formed within the cylindrical grid structure and are drawn out for focusing by the potential applied to the adjacent apertured plate. The electron beam traverses a diameter of the ion region and interacts with the neutral sample causing ionization. Ions formed inside the ion region are extracted in the direction of the neutral beam on the ionizer-quadrupole axis and through the ion optics. The sample beam from the aerodynamic source traverses the entire length of the ionizer-filter-multiplier assembly.

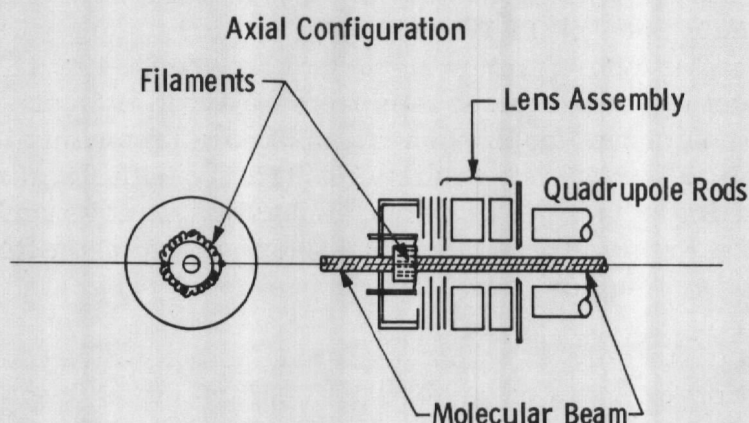


**Figure 19. Ionizer construction for the mass spectrometer assembly used in the molecular beam chamber.**

The ion optical lenses contain an important electron barrier. In a conventional ionizer, electrons from the ionizing beams can scatter from residual gas and travel along the mass filter axis. Their speed is such that they can completely traverse the mass filter during those two times in each RF cycle when the fields inside the mass filter approach zero. At the end of the quadrupole the electrons can ionize residual gases immediately before the multiplier, producing an untunable noise throughout the entire mass spectrum. However, the electron barrier in ionizers prevents such electrons from entering the mass filter in the first place, producing a significant improvement in signal-to-noise ratio.

Operation of the ion source was investigated and signal to noise maximized at the desired electron energy of 75 volts.

#### 4.3.2 Quadrupole Cracking Patterns

A difficulty encountered whenever a mass spectrometer is required to sample a multispecie gas is the extraneous signals introduced at a given

mass number due to fragmentation of heavier species in the ion source. The ensemble of mass peaks created when a molecule fragments due to an electron collision in the ion source is termed the cracking pattern. The dissociation cross section for a given molecule may be a significant percentage of the ionization cross section and hence the daughter peaks become quite large with respect to the parent. Large daughter contributions at the mass location of another parent confuses the interpretation of that particular peak. In the case of a rocket plume with a large number of species, including many light hydrocarbons resulting from fuel fragments, data interpretation may become very difficult. If the cracking patterns of most species present are known, however, a correct interpretation of a complicated mass spectra is possible. In some instances cracking may even be beneficial as in the case of  $N_2$  and CO which have the same parent mass but whose daughters allow quantitative evaluation of the mass 28 peak.

In general, the cracking patterns for most light hydrocarbons and many of the common gases have been documented as functions of electron energy by the American Petroleum Institute. It appeared from the published data (Ref. 14) that the mass spectrometer ion source could be operated at low enough electron energies to eliminate a great deal of the cracking. Since no quadrupole data were available it was necessary to obtain cracking patterns for the quadrupole system for at least representative gases and compare them to the API magnetic sector values.

Research grades of methane, acetylene, ethylene, and propylene were subjected to various ion source electron energies and the mass spectra recorded. Tables 5 through 8 present the cracking patterns of those four gases for various electron energies. Included in each table is the accepted API values for the particular gas. Although exact agreement does not exist, the standard patterns are approximated by those of the quadrupole system. The low electron energy results do indicate the feasibility of simplifying the cracking patterns.

The similarity of the quadrupole light hydrocarbon cracking patterns permitted employment of the standard patterns for data reduction. Additional gases studied (air, nitrogen, carbon monoxide, and carbon dioxide) also verified the applicability of the standard patterns.

**Table 5. Methane Cracking Patterns**

Gas: Methane, CH<sub>4</sub>  
Molecular weight: 16  
Purity: 99.98 percent

Electron Energy, v	<u>Signal Relative to Parent</u>				API Value 70
	20	50	70	100	
Mass Number					
1					0.015
12		0.015	0.025	0.045	0.030
13		0.05	0.045	0.065	0.065
14	0.003	0.125	0.115	0.130	0.014
15	0.355	0.675	0.73	0.72	0.83
16	1.0	1.0	1.0	1.0	1.0
17	0.020	0.025	0.02	0.025	0.015

**Table 6. Acetylene Cracking Patterns**

Gas: Acetylene, C<sub>2</sub>H<sub>2</sub>  
Molecular weight: 26  
Purity: 99.6 percent

Electron Energy, v	<u>Signal Relative to Parent</u>				API Value 70
	20	30	40	70	
Mass Number					
2	0.02	0.02	0.03	0.025	
12		0.005	0.03	0.035	0.02
13		0.02	0.085	0.09	0.05
14		0.01	0.02	0.02	
24		0.03	0.075	0.08	0.055
25		0.22	0.21	0.21	0.205
26	1.0	1.0	1.0	1.0	1.0
27					0.025

**Table 7. Ethylene Cracking Patterns**

Gas: Ethylene,  $C_2H_4$   
Molecular weight: 28  
Purity: 99.98 percent

Electron Energy, v	<u>Signal Relative to Parent</u>					API Value 70
	15	20	30	40	70	
Mass Number						
2			0.02	0.025	0.025	
12			0.05	0.025	0.025	
13				0.03	0.06	
14				0.08	0.075	0.06
24				0.045	0.05	0.03
25			0.03	0.05	0.07	0.105
26		0.20	0.48	0.58	0.465	0.585
27		0.215	0.52	0.59	0.465	0.605
28	1.0	1.0	1.0	1.0	1.0	1.0
29		0.02	0.02	0.02	0.02	0.02

**Table 8. Propylene Cracking Patterns**

Gas: Propylene,  $C_3H_6$   
Molecular weight: 42  
Purity: 99.99 percent

Electron Energy, v	<u>Signal Relative to Parent</u>				API Value 70
	20	30	40	70	
Mass Number					
15				0.095	0.060
19				0.21	0.005
26			0.005	0.175	0.125
27	0.155	0.665	0.56	0.686	0.495
37			0.035	0.155	0.165
38		0.04	0.14	0.285	0.255
39		0.75	0.895	0.865	0.995
40	0.200	0.405	0.335	0.355	0.40
41	0.76	1.175	1.335	1.10	1.450
42	1.0	1.0	1.0	1.0	1.0
43	0.06			0.025	0.015

### 4.3.3 Effects of Long RF Lines

One consideration that must be given to the mass spectrometer is its operation with extended line length. Standard cable lengths for most applications are approximately 10 ft, considerably less than that required for plume chamber installations such as would be necessary in the Mark I chamber. Conventional installations usually resolve H (1 amu) as the lowest detectable mass number. Because of the radio-frequency (RF) potentials required, extended cables in current commercial designs shift the operating frequency to a lower value until the lowest detectable mass number is greater than that of H<sub>2</sub> (2 amu). For most rocket fuels, hydrogen is one of the major exhaust constituents and is, therefore, of considerable interest in plume tests. Cable selection and cable routing must be chosen to minimize the capacitance loading on the RF tank circuits to ensure low mass number resolution.

A cursory experimental investigation was conducted to determine if system modifications could be performed which would allow hydrogen resolution with long RF cables (60 ft). The results of these experiments indicated that proper ion source and quadrupole operating potentials could be chosen which allow sufficient sensitivity with acceptable resolution. However, it was always observed that the operation of the mass spectrometer system in these modes was subject to be unstable and required nearly constant changing of potentials.

## 4.4 ADDITIONAL PERFORMANCE CONSIDERATIONS

Other considerations besides the probe and mass spectrometer must be made when sampling cold or hot flows from orifice-nozzle configurations. Additional effects of the gas source itself, including special pumping (such as hydrogen pumping previously considered) requirements and additional constituency changes within the plume, must be taken into account.

### 4.4.1 Frost Poisoning

The plume constituents of a typical liquid rocket engine (Table 1) are all pumpable on 20°K surfaces if CO<sub>2</sub> is added to absorb the hydrogen. The mechanism for absorption is the adsorption onto the surface and diffusion into the pores of the CO<sub>2</sub> frost where it adheres to "sites" in the frost. Gases other than hydrogen can also adsorb and diffuse into the CO<sub>2</sub> and occupy these sites, thus effectively limiting the hydrogen-pumping capacity of the frost. It is expected that the hydrocarbons with

high diffusion coefficients may "poison" the CO<sub>2</sub> frost and significantly limit the mass spectrometer probe's hydrogen-pumping capability. In an effort to investigate this effect, CO<sub>2</sub> frosts were contaminated with methane gas in molar amounts equivalent to the CO<sub>2</sub> itself. Hydrogen was bled into the probe for these frosts at measured flow rates. A comparison of the probe pressures for the contaminated frosts with those for uncontaminated frosts revealed no significant differences. The methane apparently possesses a hydrogen-pumping capability similar to CO<sub>2</sub>. Examination of the expected constituents reveals that this is true of several of the plume gases (Ref. 8) and, therefore, frost poisoning may not be a significant problem.

#### **4.4.2 Diffusive Separation in Sonic Orifice Flows**

The sonic orifice free-jet expansion is a well documented flow field (Ref. 13) which is very advantageous for calibration of instruments such as the mass spectrometer probes. Numerous experimental data presented in this report have been for sonic orifice expansions. The advantage of the field is the ability to easily determine flow-field properties by theoretical means. In sonic orifice expansions of mixtures, the reliability of these calculations is also good except in instances where diffusive separation or background gas invasion effects tend to distort the species concentrations within the jet. The first of these topics will be discussed in this section.

Sherman (Ref. 15) introduced the theory of diffusive separation in binary gas mixtures in which he expanded all the flow quantities in an asymptotic series in inverse powers of the Reynolds number. A depletion of the light species along the centerline of a free jet was predicted and has subsequently been experimentally verified (Refs. 4 and 16). The calibration gas mixtures of interest in this investigation were binary and ternary. The light specie, hydrogen, possesses a very low molecular weight and is easily separated from the remainder of the mixture. However, if nozzle (or orifice) stagnation Reynolds numbers are kept at 3,000 and above, the deviation of gas constituents from the plenum gas is negligible. In the calibration runs made using sonic orifice expansions the Reynolds number criteria was always observed, thus negating diffusive separation effects.

#### **4.4.3 Background Gas Invasion**

The premise upon which so much reliance on free-jet experiments is based is that the isentropic core of the jet is completely oblivious to the surrounding background pressure as long as the background pressure-to-jet stagnation pressure ratio is low enough to permit existence of the

jet at all. Hence a true zone of silence exists in the free jet, and the centerline flow quantities in the inviscid core are completely independent of the background pressure. Roger Campargue and his colleagues (Refs. 17 through 19) have examined molecular beams skimmed from free-jet centerlines and concluded that for given pressure ranges this is not necessarily the case. In Ref. 19 Campargue indicates that over the background pressure range of  $10^{-2}$  torr to 1 torr the free-jet shock structure is porous with respect to the background gas. It was not indicated, however, over what range of source conditions this applied. Since anticipated background pressures could reach these levels, experiments were carried out in an attempt to determine if this regime was of importance for either the cold flow calibration runs or any rocket firings which might be included in this research endeavor.

The experiments were performed in the Aerodynamic Molecular Beam Chamber using nitrogen and argon as free-jet gases. A variety of gases (argon, nitrogen, hydrogen, and some mixtures) were carefully bled into the chamber background outside the free-jet shock structure. For the source conditions of interest, no perceptible increase in background gas density along the free-jet centerline (as determined by mass sampling the skimmed centerline) was observed for various values of background pressures. It was concluded that the background invasion was of no consequence to the experiments to be conducted with the mass spectrometer sampling probes.

## 5.0 SAMPLING OF A 1-LB-THRUST MMH/ $N_2O_4$ ROCKET ENGINE

The mass spectrometer sampling probes discussed in this report were designed to sample a 75-lb liquid rocket engine in the Mark I Aerospace Environmental Chamber. It was indicated previously that the probes would be capable of sampling smaller engines operated in other vacuum chambers. A 1-lb-thrust MMH/ $N_2O_4$  engine was available for utilization in operating a mass spectrometer probe in an actual rocket exhaust environment. This engine was compatible with several available cryogenic chambers and, therefore, testing of a probe with that engine was carried out.

### 5.1 CHAMBER

The chamber selection for rocket testing the mass spectrometer probe was based on compatibility, availability, and economy. The 4-by 10-ft Research Vacuum Chamber (RVC) satisfied all three of these

criteria and was thus selected. It possessed the additional advantage of having a permanently installed electron beam fluorescence system which could assist in calibration of the mass spectrometer probe. A schematic of the 4- by 10-ft RVC and the associated rocket configuration is shown in Fig. 20.

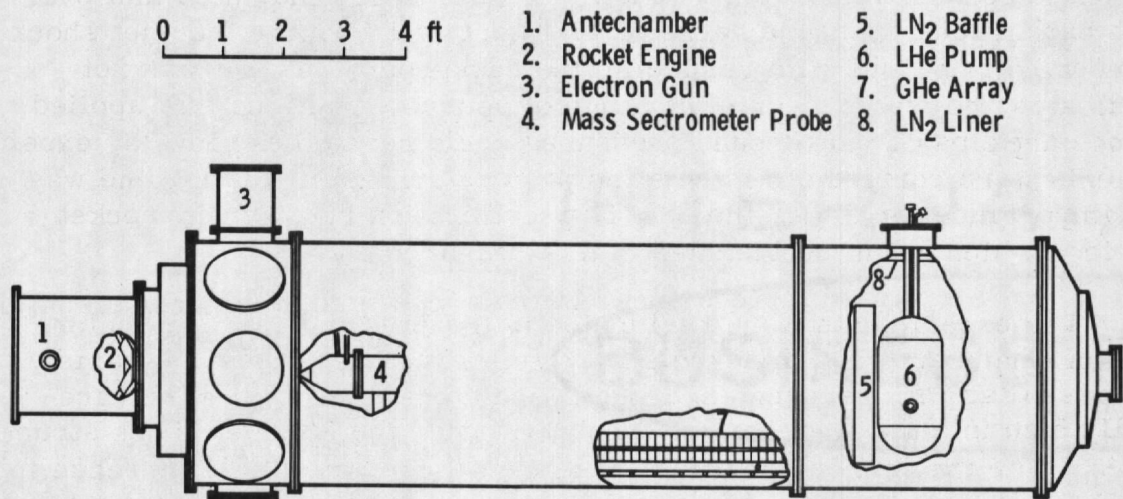


Figure 20. Schematic of 4- by 10-ft research vacuum chamber and rocket configuration.

Various additions to the conventional chamber system had to be made in order to successfully operate the 1-lb-thrust engine. These included the fuel and oxidizer supply systems, toxic vent systems, a liquid helium pump for pumping the hydrogen in the plume, and the various instrumentation for system operation.

## 5.2 PROBE SELECTION AND MODIFICATION

The two mass spectrometer probes discussed in this report were considered prototypes for a rocket exhaust-sampling probe. The experimental evaluation of the two probes determined that the flat-face probe was capable of sampling a 1-lb-thrust engine at a distance of 10.2 ft from the nozzle exit plane. This distance was not compatible with the chamber selected. The conical probe was shown to be capable of sampling plumes at impact pressures equivalent to those expected at approximately 56 in. from the rocket nozzle exit. This distance was compatible with the selected chamber; therefore, in the interest of time and economy, the readily-available conical probe was selected for sampling the 1-lb-thrust engine rocket plume.



In the process of mounting the conical probe in the 4- by 10-ft RVC it became necessary to position the probe closer than the anticipated 56 in. In order to compensate for the increased impact pressure which would exist at the lesser separation distance, it was necessary to resize the mass spectrometer probe skimmer orifice. The original orifice was 0.040 in. in diameter and the new axial distance required the orifice area to be reduced by a factor of at least  $1/3.7$ . The new skimmer orifice diameter was chosen as 0.020 in. This permitted sampling at an even smaller axial separation distance if desired.

### 5.3 ROCKET ENGINE

The 1-lb scaled thruster used in the rocket plume study was supplied originally by McDonnell Douglas for a NASA manned orbiting laboratory test. The bipropellant MMH/ $\text{N}_2\text{O}_4$  thruster was designed for both steady and pulsing operation. The engine performance was previously investigated by Marquardt Corporation personnel who found that the engine's combustion efficiency was lower than conventional (larger thrust) bipropellant engines. A schematic of the 1-lb-thrust engine is shown in Fig. 21. It consists of a single doublet, water-cooled injector head, high response solenoid valves, and two  $5\text{-}\mu$  nominal filters upstream of each valve. The nozzle and combustion chamber are an integral part, machined from molybdenum. The measured nozzle contour is shown in Fig. 22.

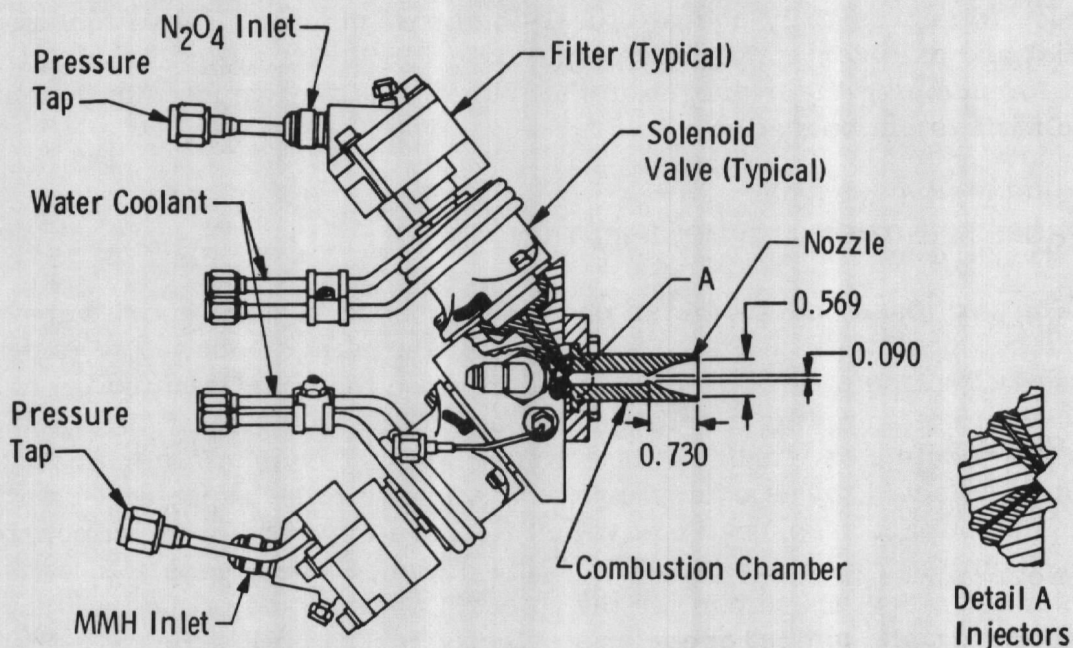


Figure 21. One-pound thrust engine and values.

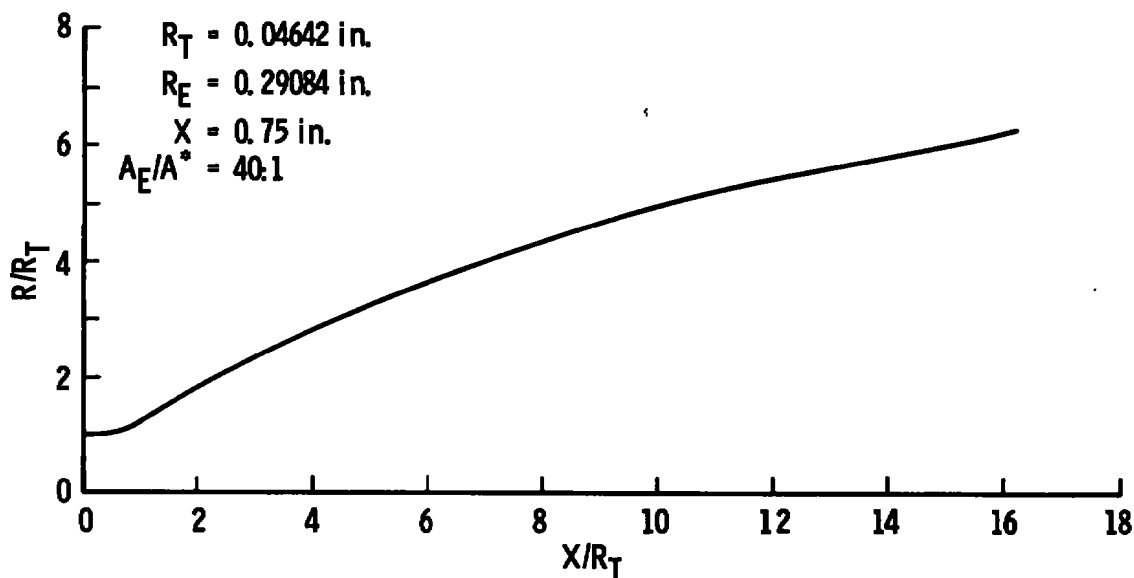


Figure 22. Nozzle contour of thruster.

The thruster design parameters and performance characteristics are shown in Table 9.

Table 9. One-Pound Rocket Engine Characteristics

Thrust	1.0 lb
Fuel	MMH
Oxidizer	$N_2O_4$
Chamber pressure	90 psi
Mixture ratio	$1.65 \pm 0.15$
Nozzle expansion ratio	40:1
Nozzle geometry	Contoured
Chamber temperature	$4,000^\circ F$
Throat diameter	0.090 in.
Nozzle exit diameter	0.569 in.
Combustion efficiency	0.830

## 5.4 FUEL AND OXIDIZER SYSTEMS

The 1-lb engine propellant system consisted of three main parts: the engine nitrogen purge, the high point bleeds, and the propellant supply system. The two propellant run tanks had capacities of approximately 1 gal each. This allowed a total operating time of approximately 1.6 hr with one propellant fill. A 20-gal water scrubber for the fuel and a 35-gal NaOH scrubber for the oxidizer were included in the system. A schematic of the propellant system is presented in Fig. 23.

The sections of fuel and oxidizer plumbing immediately adjacent to the engine were encased in a stainless steel shroud for safety purposes. The shroud was vacuum tight with a removable end flange which permitted access to the engine while the chamber was at test conditions. A photograph of the shroud, rocket engine, and some components of the propellant system is presented in Fig. 24.

The dry nitrogen pressurization system which was employed to pressurize the propellant tanks and to purge lines was also used as a cold gas calibrator for the mass spectrometer. The propellant system allowed the nitrogen to be flowed through the engine and act as a pure nitrogen gas source for sensitivity checks.

Special Omniflow<sup>®</sup> stainless steel flowmeters were installed in each side of the propellant system to permit accurate determination of the propellant flow rates. Direct measurement of the O/F ratio allowed proper adjustment of this highly significant engine parameter for altering plume mass spectra.

## 5.5 LIQUID HELIUM PUMP

Prior to attempting operation of the 1-lb thruster in the 4- by 10-ft RVC it was determined that a liquid helium pump would be necessary to handle the heat load and hydrogen gas load of the engine exhaust. The theoretical heat load from the engine may be determined from the relation

$$Q_g = \dot{m}[C_p(T_o - T_{panel}) + H_v + H_F] \quad (4)$$

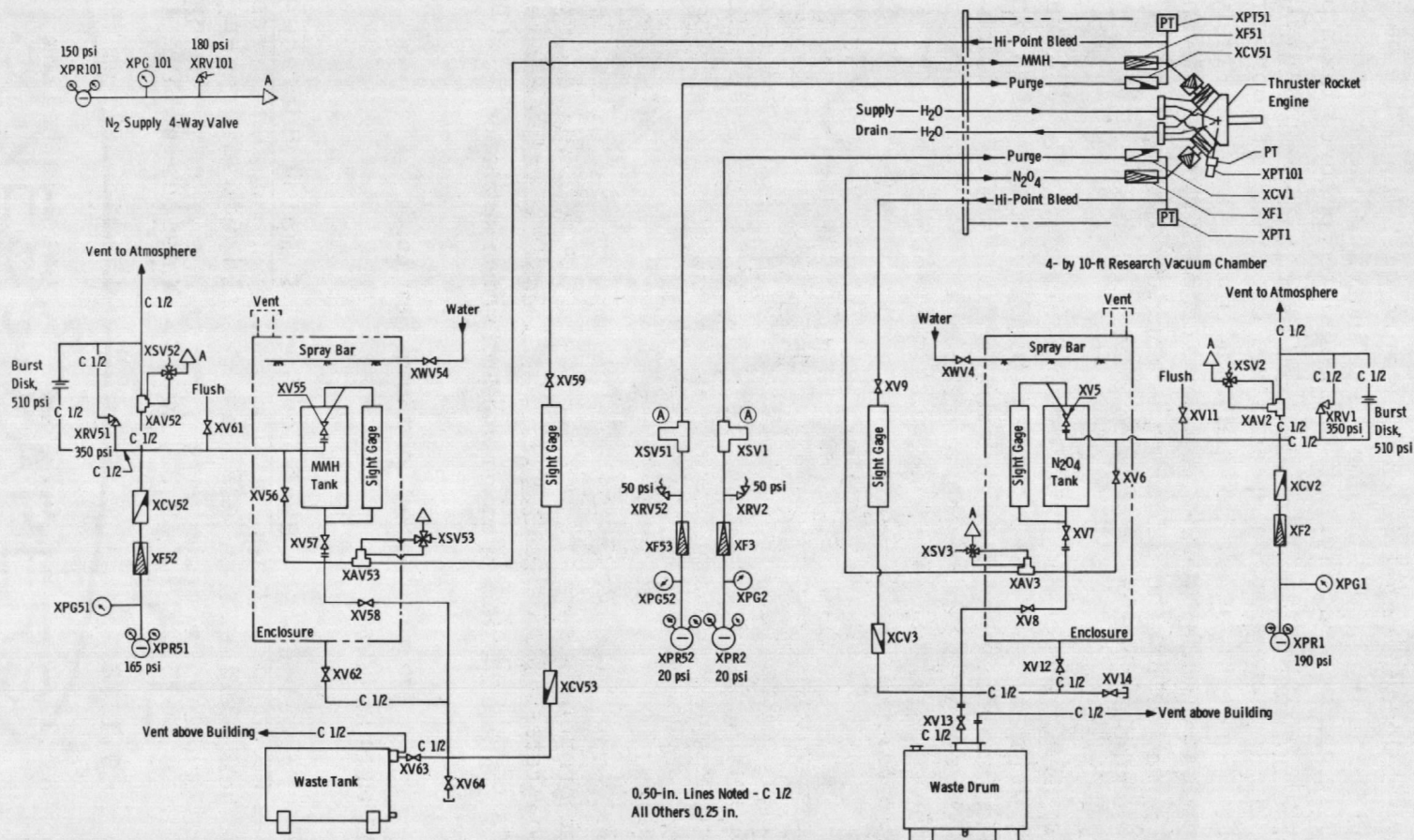


Figure 23. Schematic of rocket engine propellant system.



where  $C_p$  is the specific heat at constant pressure,  $T_{\text{panel}}$  is the temperature of the cryogenic panel which pumps the gas,  $H_V$  is the heat of vaporization and  $H_F$  is the heat of fusion. The individual heat loads of the major constituents can be obtained by using Eq. (4) for each gas. The five major constituents and their expected heat loads and pumping surfaces are given in Table 10.

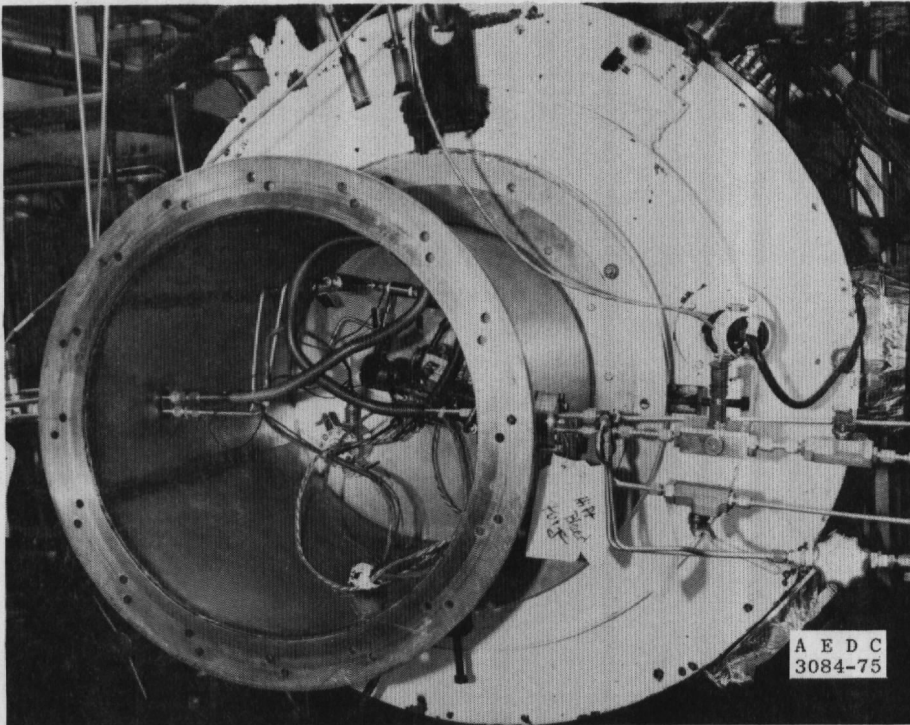


Figure 24. Rocket engine-propellant system installation.

Table 10. Rocket Constituent Heat Loads

<u>Gas</u>	<u>Mole Fraction</u>	<u>Heat Load</u>	<u>Pumping Surface</u>
H <sub>2</sub> O	0.3343	4.88 kw	Liquid nitrogen (LN <sub>2</sub> )
N <sub>2</sub>	0.3075	2.33 kw	Gaseous helium (GHe)
H <sub>2</sub>	0.1576	1.09 kw	Liquid helium (LHe)
CO	0.1287	0.84 kw	Gaseous helium
CO <sub>2</sub>	0.0401	0.21 kw	Liquid nitrogen

Since only LHe will pump hydrogen (although some of the heat load may be absorbed by the other panels) the LHe was designed to handle a 1-kw hydrogen heat load. In addition, the LHe pump must have sufficient pumping speed (surface area) to pump the hydrogen gas load of  $2.43 \times 10^{-2}$  gm/sec and maintain the necessary vacuum chamber background pressure of  $2 \times 10^{-3}$  torr.

Although the hydrogen heat and gas load made it necessary to install a LHe pump in the vacuum chamber, they were certainly not the only sources of heat loading of the liquid helium system. The extremely low temperature of liquid helium, 4.2°K, requires almost any surface in the chamber to be considered a non-negligible radiation heat source. The conduction through the chamber walls, convective heating due to gases within the chamber, and the radiation heat load from the warm surroundings must all be considered.

Since the vacuum chamber was to be evacuated to approximately  $5 \times 10^{-6}$  torr before filling of the liquid helium pump would be started, the convective heating of chamber background gases was estimated to be negligible. The conduction of heat from the chamber walls was eliminated by suspending the pump from the LHe transfer line and supporting the pump by thin stainless steel wires attached to the pump and the vacuum chamber walls. The sizing of the pump was thus dependent only on the  $H_2$  gas load and the radiation heat load from its environment.

The estimated pumping speed of hydrogen (including capture coefficient) for a liquid helium temperature surface is approximately  $10 \text{ l/sec cm}^2$ . Since the hydrogen mass flow rate is  $2.43 \times 10^{-2}$  gm/sec the total throughput (if the gas is precooled to 77°K) is 58.3 torr l/sec. The required pumping speed is given by the relation

$$S = \Pi/P_B$$

This yields a required pumping speed of  $5.83 \times 10^4 \text{ l/sec}$ , or a pump area of  $5,830 \text{ cm}^2$ .

The radiation heat load on a pump of that area may be determined from the Stefan-Boltzmann law,

$$Q_R = \epsilon \sigma A (T_w^4 - 4.2^4) \quad (5)$$

For a 300°K wall and a pump of the calculated area, Eq. (5) yields a radiation heat load of 268 joules/sec. If one determines the radiation

boiloff rate based on a heat of vaporization of 2,560 joules/l the rate is calculated to be 376 l/hr, a ridiculous amount. Hence, the pump is not feasible unless surrounded by LN<sub>2</sub> surfaces at 77°K. Under those conditions the radiation boiloff rate is reduced to 1.63 l/hr, a realistic value. Thus, the LHe pump was surrounded by LN<sub>2</sub> surfaces to reduce the radiation heat load. The boiloff per shot due to the hydrogen in the plume would be 1.28 l for a 3-sec firing.

Thus, a 37 l LHe pump was designed, built, and installed in a section of the 4- by 10-ft RVC for pumping the hydrogen gas generated during the rocket engine firings. A schematic of the liquid helium pump section is presented as Fig. 25.

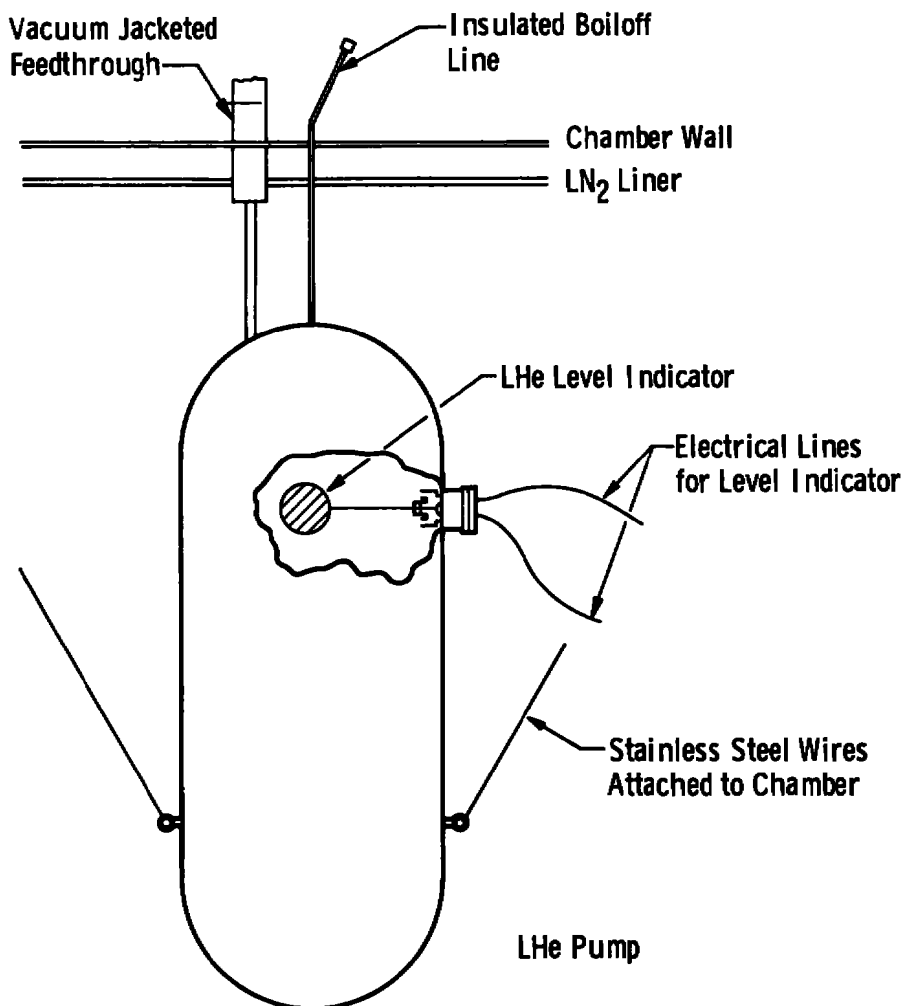


Figure 25. Liquid helium pump schematic.

## 5.6 INSTRUMENTATION

There were several facets to the instrumentation system which were taken into consideration. These were (1) the mass spectrometer system, (2) the vacuum chamber, and (3) the engine systems. Items (2) and (3) were consolidated as a composite system through the use of an online computer. This was required in order to implement as many safety precautions into the test as possible. Generally speaking, the mass spectrometer functions were separated from all others and recorded on a Visicorder® transient oscillograph. This was necessitated by the desirability of acquiring at least one mass spectra every 0.1 sec. Assuming 65 amu/sweep and 10 samples/peak, a spectra sampling rate of  $154 \mu \text{sec/sample}$  would be required exclusive of sweep samples for peak identification. Although these rates are well within the capabilities of the computer A/D conversion system, implementation of data input of other important parameters would be jeopardized. Thus, the systems were generally divided with mass spectrometer and related data recorded on the visicorder and the engine and chamber parameters recorded by a PDP-8 computer.

### 5.6.1 Mass Spectrometer System

The following items were felt to be important for spectra interpretation and engine performance evaluation:

1. electron multiplier output, high and low sensitivity,
2. mass spectrometer sweep control voltage,
3. engine combustion chamber pressure,
4. oxidizer and fuel pressure,
5. vacuum chamber pressure, and
6. probe pressure.

Only six visicorder channels were available for the mass spectrometer system so only those parameters of greatest interest for a specific run could be chosen. However, all parameters with the exception of mass spectrometer electron multiplier and sweep control voltage were duplicated within the computer data acquisition.

Several mass spectrometer parameters were not recorded automatically since they were normally fixed for optimum signal output. Normally, 0.5-ma emission current and 3,000-v multiplier voltage were



used with the exception of those runs when minor species were to be identified when a 1-ma/3,900-v combination was used.

### 5.6.2 PDP-8 Computer System

The utilization of the computer data acquisition was imperative in order to incorporate as many safety precautions into the installation as possible. There was an element of uncertainty regarding the performance of the engine and the vacuum chamber; thus, in addition to the importance of data for test purposes, many parameters were monitored so that appropriate control functions could be initiated if certain limits were exceeded. This function was usually automatic engine shutdown.

The following engine parameters were recorded:

1. fuel and oxidizer temperatures (3 each),
2. fuel and oxidizer pressures (1 each),
3. nozzle tip and combustion chamber external temperatures, and
4. fuel and oxidizer flow rates

The following chamber and vacuum instrument outputs were recorded:

1. Alphatrons (fore and aft sections),
2. General Electric ion gages (fore and aft sections),
3. General Electric ion gages (impact and static), and
4. probe ion gage.

Engine time was recorded and used as a run time limiting parameter.

As a control device, the computer was used to periodically sample critical parameters and terminate the engine firing if they were outside specified limits. Prior to a data run, those limit parameters and their values were selected and stored. Engine solenoids were energized through series contacts selected sequentially by the fuel system operator and the computer. Before the solenoids could be energized, the operator selected both fuel and oxidizer solenoids; this was followed by three passes through the computer data input sequence for limit checks. If all parameters were within prescribed limits, the computer solenoid contacts were closed, accomplishing engine ignition. If any one of the selected parameters was outside the prescribed limits, the engine was shut down. For a normal run, this was engine time read from a timer-counter. After shutdown, data acquisition was continued until the data field was filled.

Any combination of 24 parameters could be input to the computer. For the maximum number of parameters, a complete data input sequence could be completed in 30 msec. Thus, the sampling rate was determined by the number of selected input parameters, the number of storage locations in the data field ( $\approx 1,322$ ), and the desired length of run time. All parameters could be recorded in a 2.75-sec run sampling at 50 ms/sweep. After a firing, all data were recorded on magnetic tape for subsequent data reduction. In addition, tabulator printout and/or plotter/oscilloscope output could be displayed as required immediately after a run.

Other parameters were measured only to identify chamber conditions, for example, certain cryogenic temperatures and the helium liquid level in the hydrogen pump. Periphery electron beam experiments required special instrument systems, some of which did not relate directly to the rocket test. However, engine hydrogen and water species measurements were made using photon counting techniques and were recorded with the computer.

## 5.7 CALIBRATIONS

As previously noted in this report, the 4- by 10-ft RVC which was chosen for the rocket experiment had as an integral part of the chamber an electron beam fluorescence system. The electron beam fluorescence technique makes it possible to determine number densities in the free stream through optical measurements. By positioning the mass spectrometer probe on the axis of a sonic orifice free jet near the point sampled by the electron beam's optical system, a twofold calibration of the mass spectrometer system may be obtained. First, as was previously indicated, the sonic orifice expansion is so well documented that an exact axial number density variation may be calculated, thus determining the number density for the mass spectrometer sampling orifice. Second, the electron beam measurement determines the number density at a point slightly upstream of the mass spectrometer skimmer which allows an extrapolation to the number density at the skimmer entrance. This two-fold calibration technique was employed in conjunction with a 3.2-mm, thin-walled sonic orifice to calibrate the conical mass spectrometer probe signal for several plume gases. The day-to-day sensitivity changes of the mass spectrometer were monitored by flowing nitrogen through the rocket nozzle at a given flow rate and monitoring the mass 28 signal. The changes in signal level indicated the sensitivity change.

Figures 26 through 28 present the calibration curves for nitrogen, carbon monoxide, and hydrogen at mass spectrometer settings used

during later engine firings. Due to the previously discussed difficulties encountered with hydrogen detection, two hydrogen calibration curves were needed. Figure 29 indicates the increased signal levels obtained with higher electron multiplier voltage. The calibration curves are presented as functions of sonic orifice source pressure, the original data. Conversion to number density is accomplished easily by means of the far-field approximation

$$n/n_o \cong \left[ \frac{(\gamma-1)}{2} A^2 \right]^{-1/\gamma-1} \left( \frac{X}{D} \right)^{-2}$$

where A is a previously given constant. In terms of source pressure and the calibration conditions this yields, for  $\gamma = 1.4$ ,

$$n = 7.91 \times 10^{10} P_o \text{ cm}^{-3}$$

where  $P_o$  must be expressed in torr. The large dynamic range of the mass spectrometer probe is indicated by the extremely low  $P_o$  values for which meaningful data are attainable.

## 5.8 CHAMBER AND ENGINE PERFORMANCE

Details of the 4- by 10-ft RVC and the 1-lb-thrust MMH/ $N_2O_4$  rocket engine (Fig. 20) have previously been presented in this report. Proper mass sampling of the engine was predicated upon the rocket exhaust performing as a free jet, hence the chamber pressures had to be low enough to permit a free-jet structure of sufficient size. From Eq. (3), Section 2.4, it may be determined that the vacuum chamber background pressure must be maintained below  $2.5 \times 10^{-2}$  torr to permit a proper free-jet structure to be formed. Fig. 30 presents a plot of the vacuum chamber pressure as a function of time for several runs. The pressure was measured with an alphasatron gage behind the rocket engine. The alphasatron was located on a warm wall and was partially open to directed flow (backflow) from the engine. When an estimated gage factor is included in the data the pressure remains below the required 25.0  $\mu\text{Hg}$  level.

The engine performance was primarily monitored through the measurement of combustion chamber pressure and the mass spectra. Due to the small pressure tap and plumbing between the combustion chamber and pressure transducer, the transducer output lagged the actual combustion chamber pressure by several milliseconds. Since run times were considerably longer than the lag time, the steady pressure was, nevertheless, recorded correctly. Figure 31 presents the measured combustion chamber pressure for three O/F ratios. The oxidizer mass flow

rate was held constant during these runs. The oxidizer solenoid value led the fuel valve on opening by 10 msec and lagged the fuel solenoid valve by 10 msec on closing. This ensured that only quantities of frozen oxidizer and no frozen fuel were cryopumped in the chamber. This permitted warmup of the cryogenic systems with little concern over reactions taking place on the chamber walls.

## 5.9 PROBE EVALUATION

The conical mass spectrometer probe was mounted in the 4- by 10-ft RVC at a distance of 91 cm, 63 nozzle exit diameters downstream of the 1-lb-thrust engine nozzle exit. The engine was operated at several O/F ratios for a variety of run times. The following sections discuss the probe performance and the results of those runs.

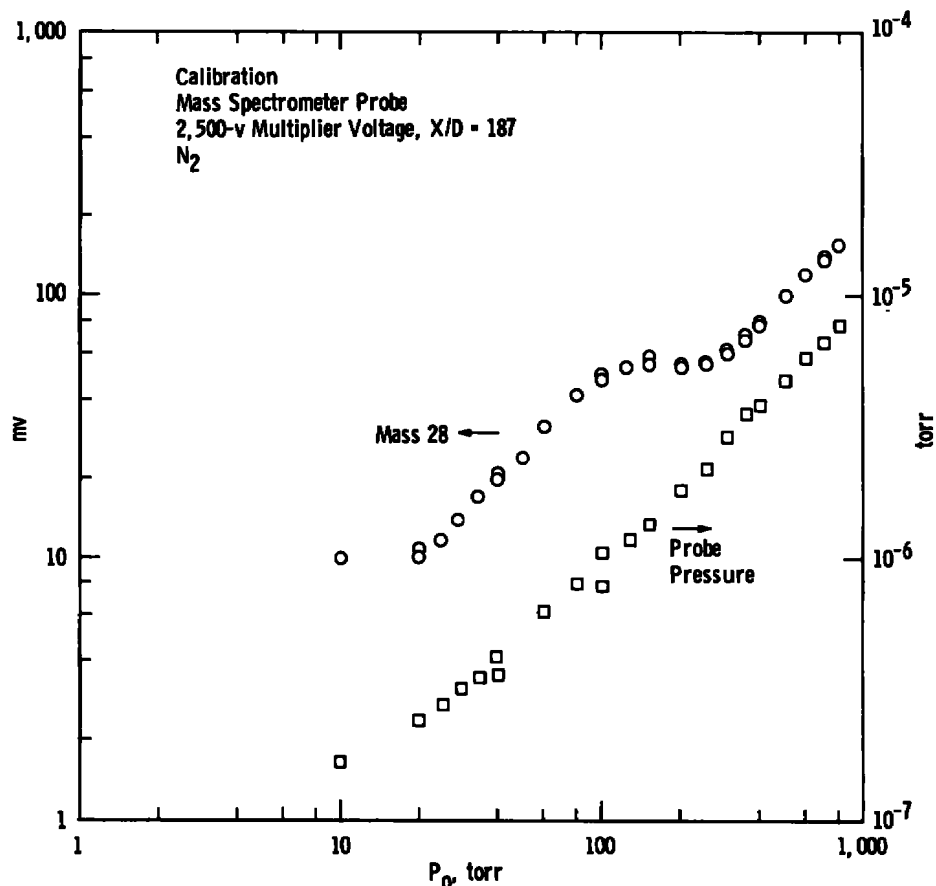


Figure 26. Nitrogen calibration.

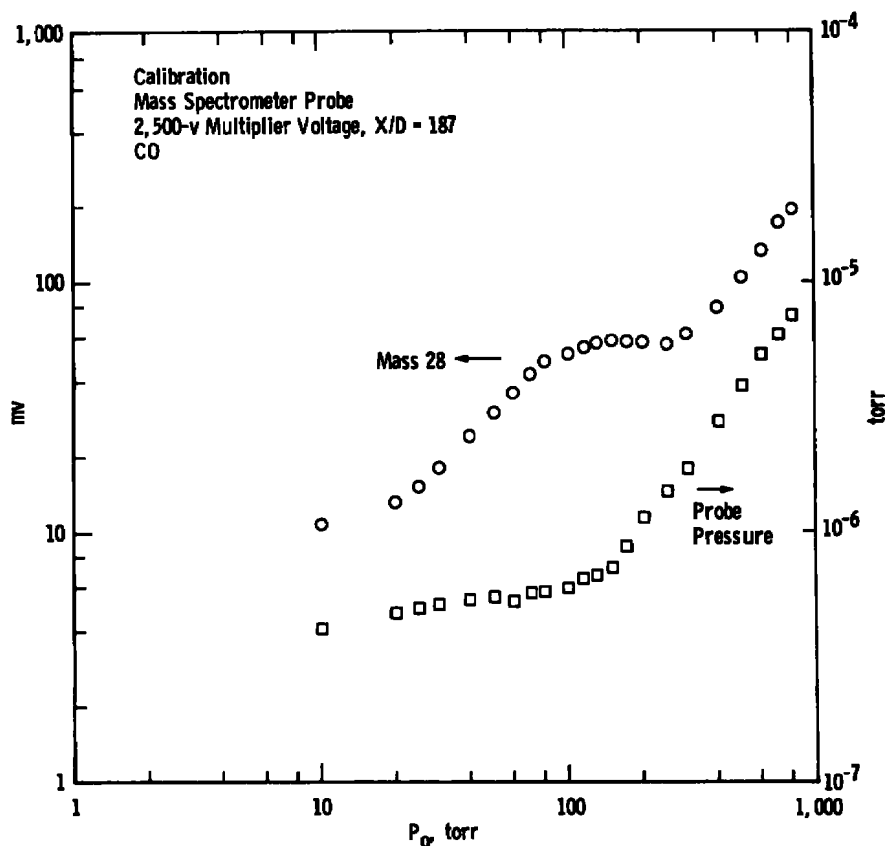


Figure 27. Carbon monoxide calibration.

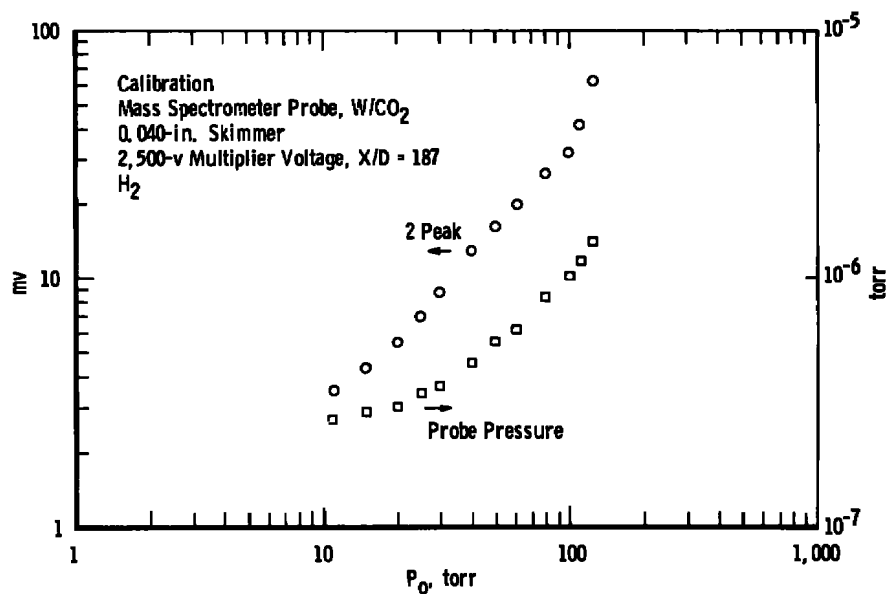


Figure 28. Hydrogen calibration, 2,500-v multiplier voltage.

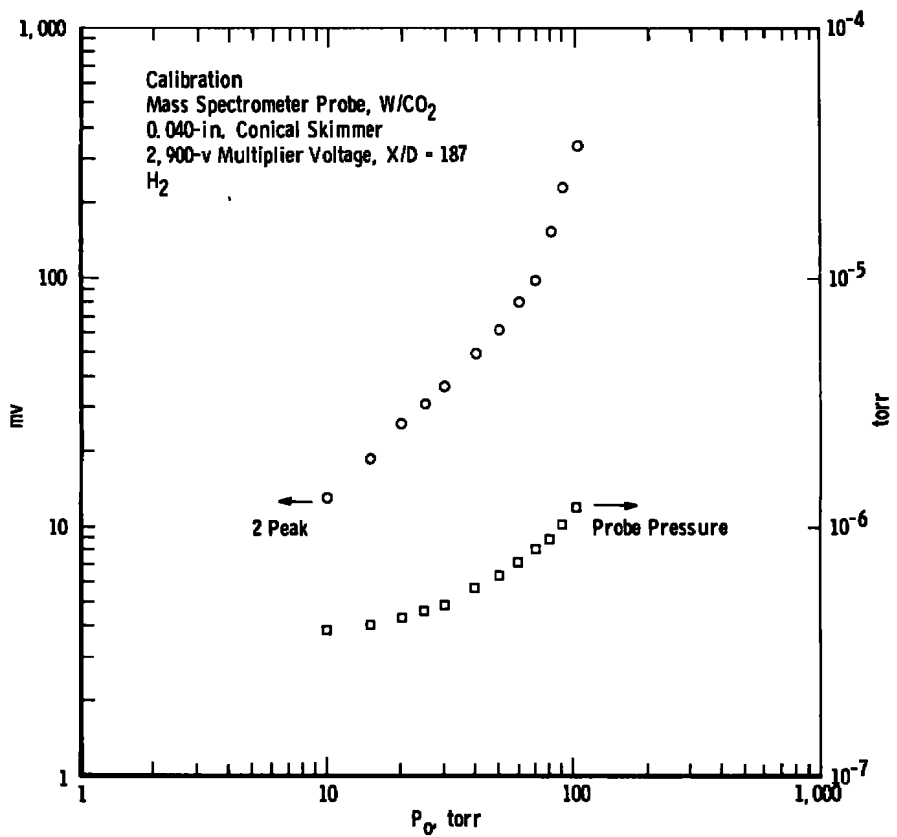


Figure 29. Hydrogen calibration, 2,900-v multiplier voltage.

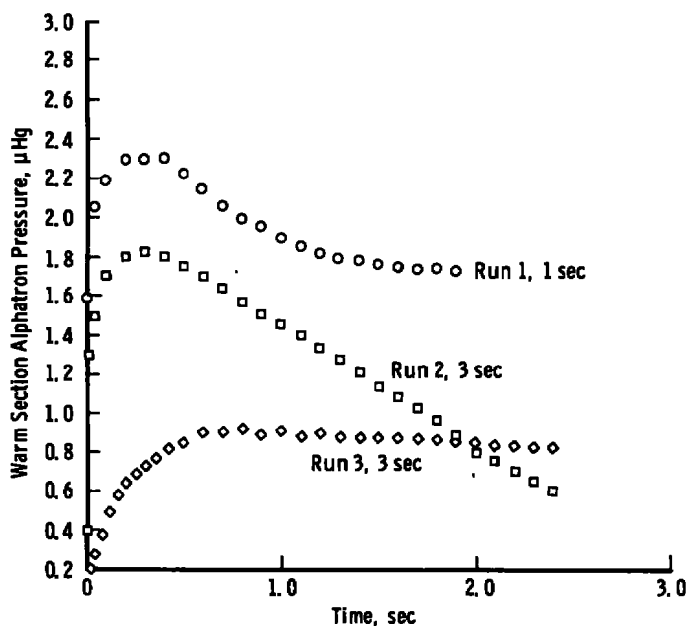


Figure 30. Vacuum chamber pressure temporal behavior.

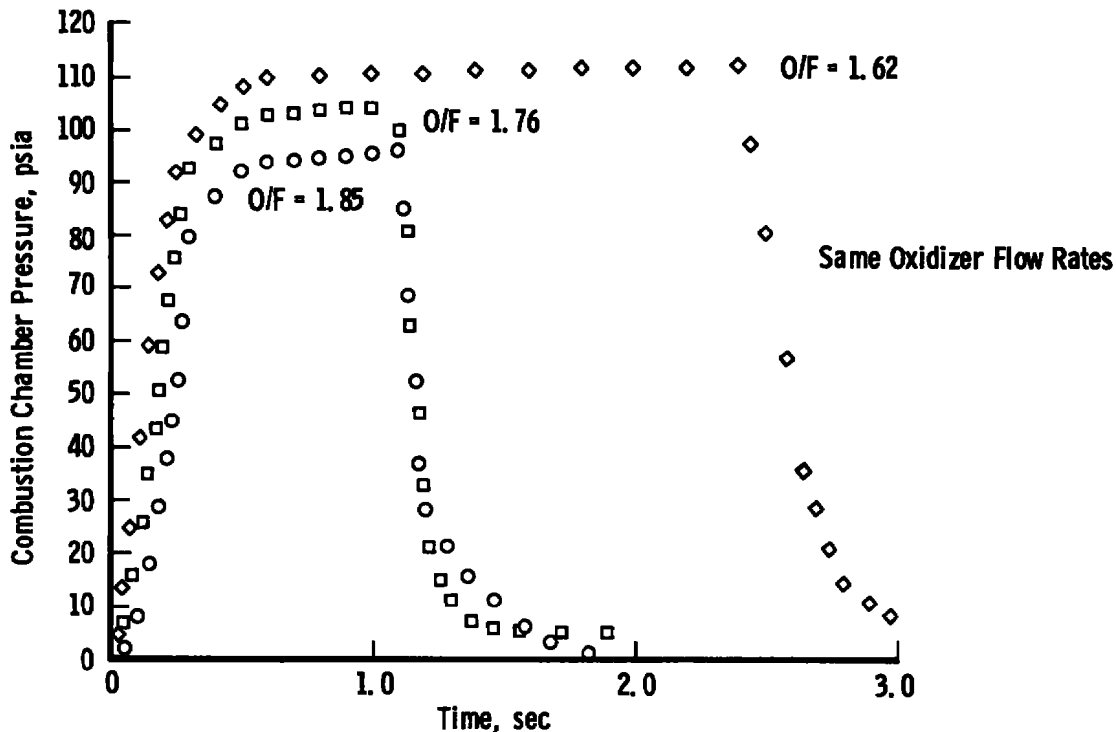


Figure 31. Combustion chamber pressure for three O/F ratios.

### 5.9.1 Probe Pumping

The mass spectrometer probe pressure was monitored during engine firings by a Veeco® ionization gage installed on the probe rear plate. The only significant variables in the pressure variation for different engine firings were the firing time and the quality of the internal  $\text{CO}_2$  frost used for hydrogen pumping. Although additional  $\text{CO}_2$  was usually deposited prior to each firing, the ability to pump the hydrogen degraded with each successive run. Typical behavior of the probe pressures during a sequence of firings is presented in Fig. 32. For each successive firing, the probe base pressure (before engine operation) is higher and so are the pressure levels throughout the firing. From previous mixture experiments, it was determined that data for probe pressures above  $5 \times 10^{-6}$  torr were questionable with respect to hydrogen measurements but were reasonably accurate for other species. It is, therefore, necessary to examine the probe pressure data before implying the significance of hydrogen number density measurements.

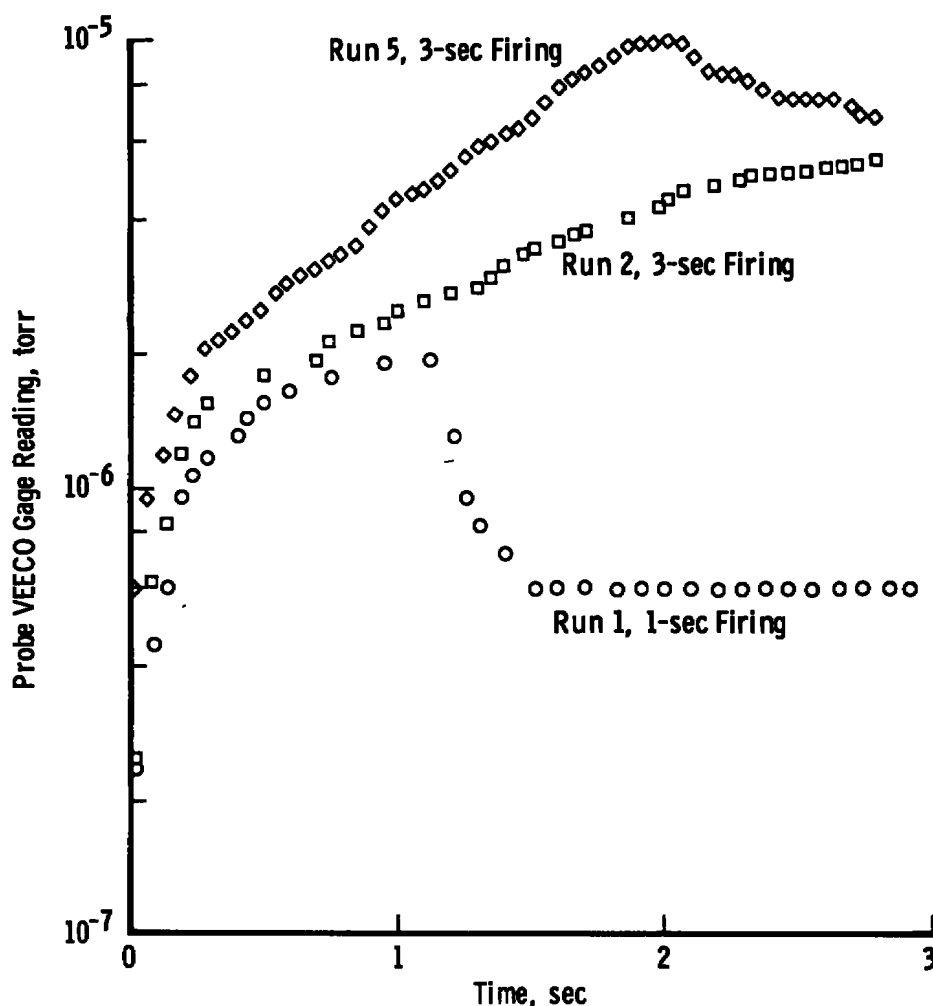


Figure 32. Probe pressure during rocket firings.

### 5.9.2 Major Species

The major species present in an equilibrium MMH/ $\text{N}_2\text{O}_4$  exhaust plume with an O/F ratio of 1.60 were listed in Table 1. An absolute measurement of the constituency of the 1-lb-thrust engine exhaust was attempted with the mass spectrometer probe for several O/F ratios. The O/F ratio was varied by controlling the fuel tank feed pressure. Therefore, except for small flow-rate changes due to combustion chamber pressure fluctuations, the oxidizer flow rate was the same for all runs. Figure 33 is an example of the oscillograph output for a particular run (O/F = 1.76). The mass sweep, combustion chamber pressure, and mass spectra for two sensitivity ranges are indicated. Figure 34 represents the variation of signal from a combustion product,  $\text{H}_2\text{O}$ , and an oxidizer



product, NO, as functions of O/F ratio. The signals are normalized with respect to the mass 28 signal for each run. Although significant scatter is evident, the combustion product signal tends to drop slightly with increasing O/F ratio while the oxidizer product increases significantly. The slight drop in mass 18 to mass 28 ratio at higher O/F ratios is due to the decrease in available fuel to support combustion. The mass 30 signal to mass 28 signal increases with O/F due to the increased amount of  $N_2O_4$  available for cracking.

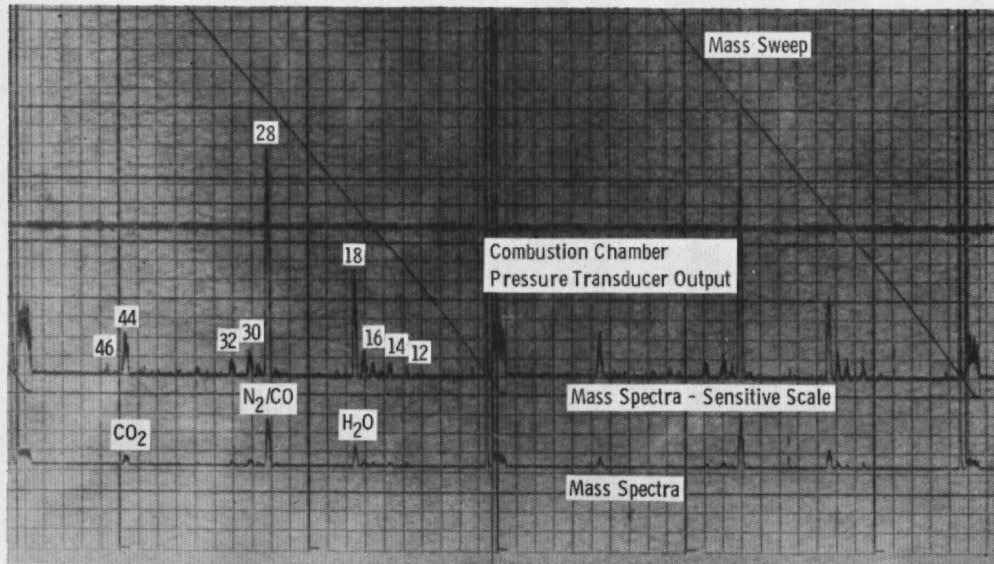


Figure 33. Typical rocket exhaust mass spectra.

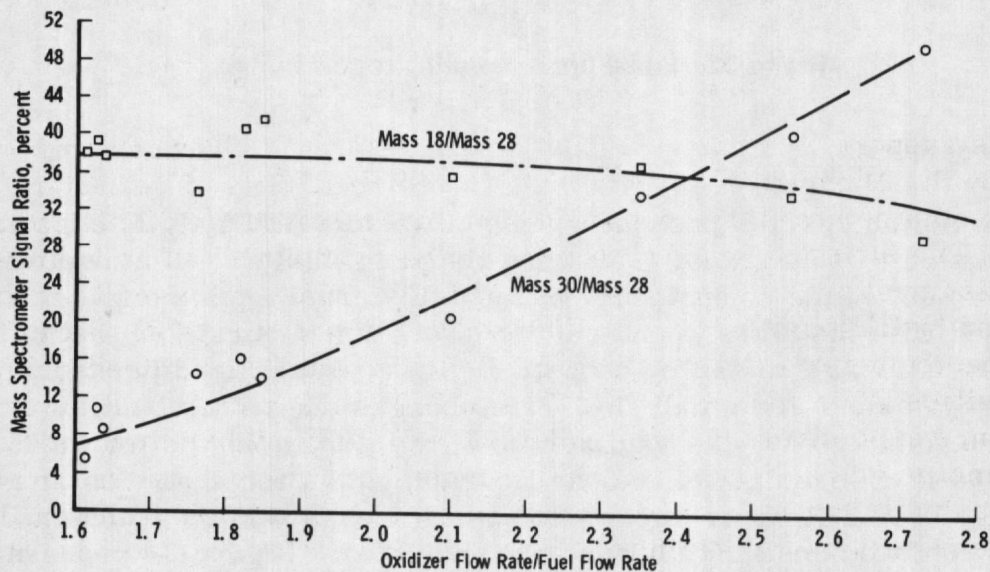


Figure 34. Variation of species with O/F ratio.

Table 11 presents the measured values of major specie number densities at an O/F ratio of 1.62. Use of the mass spectrometer calibrations, measured cracking patterns, and tabulated ionization cross sections (Ref. 20) were employed in the compilation of Table 11. A correction for nonlinear multiplier response was also included. A comparison of Table 11 and Table 1 reveals that the combustion is less than completely efficient (e.g., the  $\text{H}_2\text{O}$  mole fraction).

Table 11. Measured Species Concentrations (O/F = 1.62)

Component	Measured No. Density ( $\text{cm}^{-3}$ )	Mole Fraction of Major Species
$\text{H}_2\text{O}$	$2.97 \times 10^{12}$	0.153
$\text{N}_2/\text{CO}$	$9.9 \times 10^{12}$	0.511
$\text{H}_2$	$1.5 \times 10^{12}$	0.077
$\text{CO}_2$	$1.63 \times 10^{12}$	0.084
OH	Trace	
H	$1.27 \times 10^{12}$	0.066
$\text{O}_2$	$7.59 \times 10^{11}$	0.039
NO	$4.24 \times 10^{10}$	0.0022
O	$6.95 \times 10^{10}$	0.0036

This supports the poor combustion efficiency (0.83) reported for the engine by the Marquardt Corporation. More reliability of quantitative data could be obtained from the probe through more exacting calibration techniques. The electron beam system which was employed as an additional calibration system for the mass spectrometer probe was used to measure water and hydrogen number densities in the plume. Extrapolated to the mass spectrometer axial location the electron beam determined the number densities to be  $5.23 \times 10^{12} \text{ cm}^{-3}$  and  $2.02 \times 10^{12} \text{ cm}^{-3}$  for water and hydrogen, respectively. These values are slightly higher than the mass spectrometer values, but the ratios between the two species for both instruments basically agree. More precise mass spectrometer probe calibrations are necessary to obtain exact quantitative data. Regardless, the major specie data do indicate the probe's ability to make quantitative major specie measurements in a rocket exhaust plume.

### 5.9.3 Minor Species

In order to obtain minor specie measurements it was necessary that the mass spectrometer gain be set much higher than what had been useful in making major specie measurements. This resulted in losing some of the major specie data for particular runs due to too-high signal levels. If necessary, this loss of data could be avoided through the use of a mass switching technique.

Figure 35 presents a typical oscillograph trace for a minor specie data run. The large number of peaks which are present may be contrasted with the relatively few peaks observable in Fig. 33. Practically all mass numbers from 12 to 53 are shown in Fig. 35. This again emphasizes the complicated spectra of such a rocket exhaust and the large dynamic range of the mass spectrometer. Table 12 presents a tentative list of the principal ions identified in the spectra of Fig. 35. Quantitative interpretation of the data was not attempted. The identification of all peaks is difficult but most unidentified peaks in Table 12 (designated by a U) can be attributed to cracked pump oil present in the vacuum chamber.

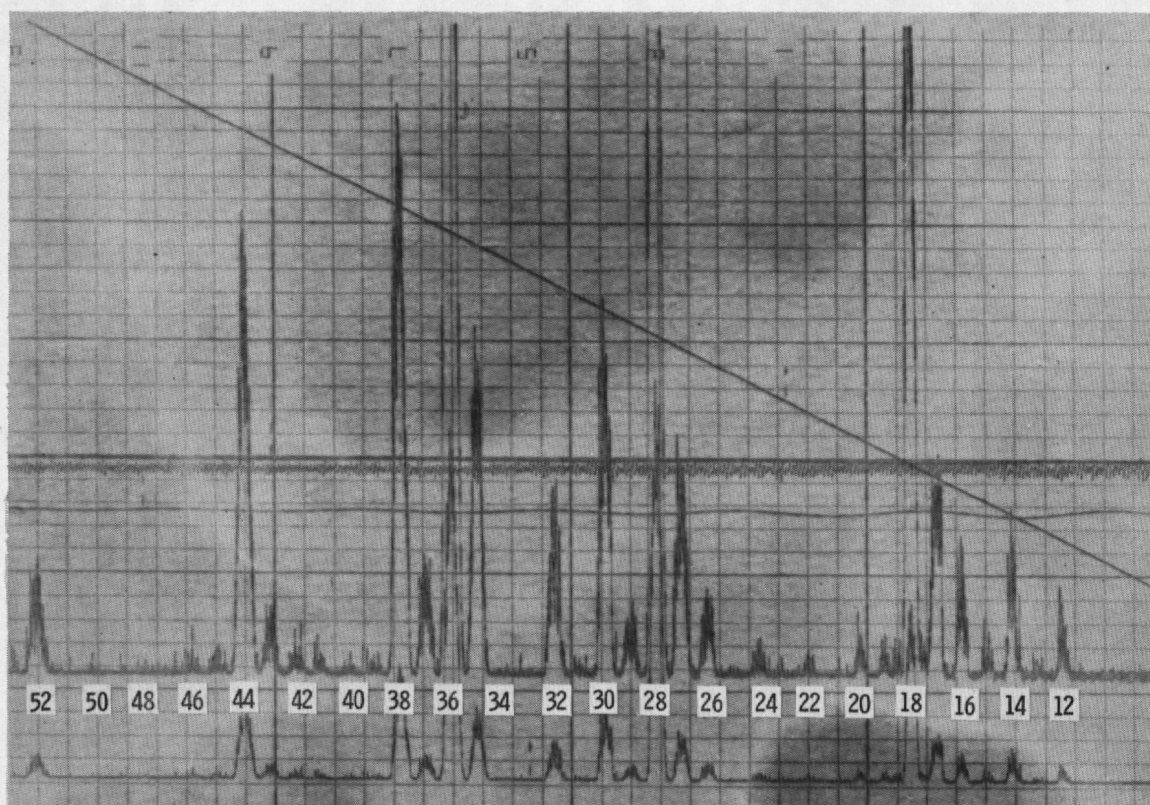


Figure 35. Minor species mass spectra.

The helium listed was due to a very small leak in the gaseous helium refrigeration system. It should be noted that the spectra is of sufficient quality to allow relative comparison of minor species for different operating conditions, although quantitative evaluation of an individual peak would be extremely difficult.

Table 12. Identified Mass Numbers in MMH/N<sub>2</sub>O<sub>4</sub> Exhaust

Specie	Mass No.	Specie	Mass No.
H <sup>+</sup>	1	NO <sup>+</sup> , CH <sub>3</sub> NH <sup>+</sup>	30
H <sub>2</sub> <sup>+</sup>	2	NHNH <sub>2</sub> <sup>+</sup>	31
He <sup>+</sup>	4	O <sub>2</sub> <sup>+</sup>	32
C <sup>+</sup>	12	U	35
CH <sup>+</sup>	13	U	36
N <sup>+</sup>	14	U	37
CH <sub>3</sub> <sup>+</sup> , NH <sup>+</sup>	15	C <sub>3</sub> H <sub>2</sub> <sup>+</sup>	38
O <sup>+</sup> , NH <sub>2</sub> <sup>+</sup>	16	C <sub>3</sub> H <sub>3</sub> <sup>+</sup>	39
NH <sub>3</sub> <sup>+</sup> , OH <sup>+</sup>	17	CN <sub>2</sub> <sup>+</sup>	40
H <sub>2</sub> O <sup>+</sup>	18	CHN <sub>2</sub> <sup>+</sup>	41
H <sub>2</sub> O <sup>+</sup>	19	CH <sub>2</sub> N <sub>2</sub> <sup>+</sup>	42
U	20	CH <sub>3</sub> N <sub>2</sub> <sup>+</sup>	43
CO <sub>2</sub> <sup>++</sup>	22	CO <sub>2</sub> <sup>+</sup> , CH <sub>3</sub> N <sub>2</sub> H <sup>+</sup>	44
U	24	CH <sub>3</sub> NHNH <sup>+</sup>	45
CN <sup>+</sup>	26	NO <sub>2</sub> <sup>+</sup> , CH <sub>3</sub> NHNH <sub>2</sub> <sup>+</sup>	46
CNH <sup>+</sup>	27	C <sub>2</sub> H <sub>4</sub> <sup>+</sup>	50
N <sub>2</sub> <sup>+</sup> , CO <sup>+</sup>	28	C <sub>4</sub> H <sub>4</sub> <sup>+</sup>	52
	29	U	53

#### 5.9.4 Velocity Distributions

Time of flight velocity distribution measurements using the metastable technique were attempted during the 1-lb engine firings. The mass spectrometer configuration was unchanged from the mass sampling runs except for the electronic setup and the electron multiplier configuration. The ion source was operated as an electronic chopper which produced ions and metastable molecules. The metastable molecules, unlike the ions, are unaffected by the electric fields within the spectrometer. The quadrupole section was operated at a resolution such that no ions would

traverse the pole section at all, thus only metastable molecules reached the multiplier section. The normally paraxial multiplier was rotated onto the spectrometer centerline and served as a metastable signal detector to give the velocity distribution's temporal waveform. A complete description of the metastable time of flight technique may be found in Refs. 2 and 5.

Unfortunately, the velocity distribution measurements were attempted near the end of the test matrix. In the interim of time between the mass sampling measurements and velocity distribution measurements the expander in the GHe refrigeration system required replacement. The new expander did not operate as well as the previous one, and consequently it became impossible to cool the mass spectrometer probe to the previously attainable temperatures. An associated loss of pumping in the probe, accompanied with high ( $10^{-5}$  torr) pole section pressures, resulted. The high pressure in the quadrupole section severely reduced any chances of obtaining velocity distributions in the plume. Several efforts were made, but all were unsuccessful.

## 6.0 SUMMARY AND CONCLUSIONS

Two cryogenically cooled mass spectrometer probes, one a flat-faced probe with a 2-mm cryogenic skimmer and the other a conical-faced probe with a heated, 20-deg half-angle, conical skimmer were designed and built to perform future measurements of the species concentrations in the far field of a rocket exhaust plume of a 75-lb-thrust bipropellant (MMH and  $N_2O_4$ ) liquid rocket engine.

Preliminary evaluation of the two probes revealed the flat-face probe to be incapable of sampling at a reasonable axial position in the exhaust plume of a 75-lb rocket engine. However, the flat-face probe could be expected to perform properly in the exhaust plume of a 1-lb thruster if operated at chamber altitude levels sufficient to permit extreme far-field measurements. The discrepancy in the design and operating characteristics is associated with the inability to insure sufficient coolant flow within the probe. The conical probe was found to be capable of operating for certain conditions in the environment of a 75-lb engine. Its improved performance relative to the flat-faced probe is associated with its larger pumping area and a less restricted coolant flow system.

The conical probe was evaluated in the exhaust plume of a 1-lb bipropellant (MMH/ $N_2O_4$ ) rocket engine at a location approximately 63 nozzle

diameters downstream of the nozzle exit. The following concluding observations may be made:

1. The probe-pumping system is capable of maintaining the high vacuum conditions necessary for mass spectrometer operation.
2. Acceptable instrument response time and sensitivity are obtainable, the corrosive environment not significantly affecting the mass spectrometer sensitivity.
3. Reasonable mass spectrums of the rocket exhaust constituents can be obtained with quantitative measurement of major species.
4. Minor constituents can be determined by use of the probe with relative comparisons being possible in some instances. Quantitative measurement is not obtainable with the present system.
5. Velocity distribution measurements are unobtainable with the present configuration, but increased probe pumping could permit employment of the metastable time-of-flight technique.
6. For the probe operating conditions in the 1-lb engine evaluation, the effects discussed in Section 2.3 of this report were determined to be of little or no consequence.

The most serious hindrance to quantitative measurements with the present probe resulted from the lack of reliable and extensive calibrations. These data could be obtained, however, through the extensive use of sonic orifice calibration experiments similar to those discussed in this report.

The primary probe limitation was the inability to handle high impact pressure levels. A correction for this shortcoming is obtainable through probe redesign to ensure maximum coolant flow rate through the probe. The conical probe was determined to be greatly superior to the flat-faced probe due to the higher coolant flow rates and increased pumping of that system. The pumping breakdown experienced by the flat-faced probe was not as serious a problem to the conical probe, and conical probes do appear much better suited to sampling the high mass flows present in rocket engine exhaust plumes.



## REFERENCES

1. Boynton, Fred P. "Rocket Plume Radiance. Part IV. Studies of Carbon Particles Formed by Small, Hydrocarbon-Fueled Rocket Engines." ERR-AN-007, Convair Astronautics Div., No. AF 19 (604)-5554, April 7, 1960.
2. Powell, H. M., Hill, D. W., and Whitfield, D. L. "Evaluation of a Mass Spectrometer Probe for Density and Velocity Distribution Measurements in a Rocket Exhaust Plume." AEDC-TR-71-135 (AD729206), September 1971.
3. Chow, R. R. "On the Separation Phenomenon of Binary Gas Mixtures in an Axisymmetric Jet." University of California at Berkeley, Technical Report No. HE-150-175, November 1959.
4. Rothe, D. E. "Electron Beam Studies of the Diffusive Separation of Helium-Argon Mixtures in Free Jets and Shock Waves." University of Toronto, UTIAS Report No. 114, July 1966.
5. Benek, J. A., Busby, M. R., and Powell, H. M. "Technique for the Analysis and Computerized Data Reduction of Time-of-Flight Distributions of Free-Jet Expansions." AEDC-TR-70-84 (AD712372), October 1970.
6. Stephenson, W. B. "A High-Energy Molecular Beam Facility Adapted to Satellite Test and Development." AEDC-TR-73-197 (AD774593), February 1974.
7. Bossel, U. "Investigation of Skimmer Interaction Influences on the Production of Aerodynamically Intensified Molecular Beams." University of California at Berkeley, College of Engineering Report No. AS-68-6, August 1968.
8. Templemeyer, K. E. "Sorption Pumping of Hydrogen by Cryodeposits - Sorption Capacity Measurement." AEDC-TR-69-266 (AD700980), February 1970.
9. Lewis, C. H., Jr. and Carlson, D. J. "Normal Shock Location in Underexpanded Gas and Gas-Particle Jets." AIAA Journal, Vol. 2, No. 4, April 1964, pp. 776-777.
10. Bailey, A. B. "Effects of Condensation on Gas Velocity in a Free-Jet Expansion." AEDC-TR-73-93 (AD762503), June 1973.

11. Limbaugh, C. C., Lewis, J. W. L., Kinslow, M., et al.  
"Condensation of Nitrogen in a Hypersonic Nozzle Flow Field." AEDC-TR-74-31 (AD919337L), May 1974.
12. Hagena, O. F. and Obert, W. "Cluster Formation in Expanding Supersonic Jets: Effect of Pressure, Temperature, Nozzle Size, and Test Gas." The Journal of Chemical Physics, Vol. 56, No. 5, March 1972, pp. 1793-1802.
13. Ashkenas, H. and Sherman, F. S. "The Structure and Utilization of Supersonic Free Jets in Low Density Wind Tunnels." Rarefied Gas Dynamics (J. H. de Leeuw, Editor), Vol. II, pp. 84-105, Academic Press, New York, 1966.
14. Biguenet, Ch. "Spectrométrie de masse dans l'analyse des gaz résiduels." Le Vide, Vol. 27, No. 159-160, Mai-Juin-Juillet-Auot 1972.
15. Sherman, F. S. "Hydrodynamical Theory of Diffusive Separation of Mixtures in a Free Jet." Physics of Fluids, Vol. 8, No. 5, May 1965.
16. Anderson, J. B. "Separation of Gas Mixtures in Free Jets." A.I.Ch.E. Journal, Vol. 13, No. 6, November 1967, pp. 1188-1192.
17. Campargue, R. "Aspiration d'un gaz pur a travers une structure de choc de jet libre." C. R. Acad. Sc. Paris, t. 268, p. 1427-1430, 9 Juin 1969.
18. Campargue, R. "Facteurs de dégradation dominants dans la production de jets moléculaires supersoniques." Entropie, No. 30, Novembre-December 1969.
19. Campargue, R. "Aerodynamic Separation Effect on Gas and Isotope Mixtures Induced by Invasion of the Free Jet Shock Wave Structure." Journal of Chemical Physics, Vol. 52, No. 4, February 1970, pp. 1795-1802.
20. Reed, R. I. Ion Production by Electron Impact, Academic Press, London 1962.



## NOMENCLATURE

$A_{\text{pump}}$	Internal probe-pumping area
$C_p$	Specific heat at constant pressure
$D$	Sonic orifice diameter
$D_e$	Nozzle exit diameter
$D_{\text{SK}}$	Skimmer diameter
$H_F$	Heat of fusion
$H_V$	Heat of vaporization
$K_n$	Knudsen number
$M$	Mach number
$\dot{m}$	Mass flow rate
$n$	Number density
$P_B$	Background pressure
$P_C$	Combustion chamber pressure
$P_i$	Impact pressure
$P_p$	Probe internal pressure
$P_s$	Static pressure
$P_o$	Stagnation chamber pressure
$Q_g$	Gas heat load
$Q_R$	Radiation heat load
$R$	Gas constant
$r_e$	Nozzle exit radius
$S$	Pumping speed
$S_1$	Pumping speed of $H_2$ for $CO_2$ on 12°K surface
$T_c$	Combustion chamber temperature
$T_{\text{panel}}$	Cryogenic panel temperature
$T_w$	Wall temperature
$T_o$	Stagnation temperature

$X$	Distance from nozzle exit to measurement point
$X'_0$	Virtual source displacement
$\gamma$	Specific heat ratio
$\epsilon$	Emissivity
$\lambda$	Mean free path
$\Pi$	Throughput
$\sigma$	Stefan-Boltzmann constant
$\omega$	Viscosity law exponent

## SUBSCRIPTS

$c$	Combustion chamber
$e$	Nozzle exit
$ref$	Reference
$s$	Static
$SK$	Skimmer
$o$	Stagnation
$\infty$	Free Stream